Eocene Loranthaceae pollen revives the Gondwana breakup hypothesis for the family (#15035)

First submission

Please read the **Important notes** below, the **Review guidance** on page 2 and our **Standout reviewing tips** on page 3. When ready **submit online**. The manuscript starts on page 4.

Important notes

Editor

Kenneth De Baets

Files	11 Figure file(s) 4 Table file(s) 7 Raw data file(s) Please visit the overview page to **download and review** the files not included in this review PDF.
Declarations	No notable declarations are present

Review guidelines

Please read in full before you begin

How to review

When ready **submit your review online**. The review form is divided into 5 sections. Please consider these when composing your review:

1. **BASIC REPORTING**
2. **EXPERIMENTAL DESIGN**
3. **VALIDITY OF THE FINDINGS**
4. General comments
5. Confidential notes to the editor

You can also annotate this PDF and upload it as part of your review

To finish, enter your editorial recommendation (accept, revise or reject) and submit.

BASIC REPORTING

- Clear, unambiguous, professional English language used throughout.
- Intro & background to show context. Literature well referenced & relevant.
- Structure conforms to **PeerJ standards**, discipline norm, or improved for clarity.
- Figures are relevant, high quality, well labelled & described.
- Raw data supplied (see **PeerJ policy**).

EXPERIMENTAL DESIGN

- Original primary research within **Scope of the journal**.
- Research question well defined, relevant & meaningful. It is stated how the research fills an identified knowledge gap.
- Rigorous investigation performed to a high technical & ethical standard.
- Methods described with sufficient detail & information to replicate.

VALIDITY OF THE FINDINGS

- Impact and novelty not assessed. Negative/inconclusive results accepted. *Meaningful* replication encouraged where rationale & benefit to literature is clearly stated.
- Data is robust, statistically sound, & controlled.
- Conclusions are well stated, linked to original research question & limited to supporting results.
- Speculation is welcome, but should be identified as such.

The above is the editorial criteria summary. To view in full visit **https://peerj.com/about/editorial-criteria/**

7 Standout reviewing tips

The best reviewers use these techniques

Tip	*Example*
Support criticisms with evidence from the text or from other sources	*Smith et al (J of Methodology, 2005, V3, pp 123) have shown that the analysis you use in Lines 241-250 is not the most appropriate for this situation. Please explain why you used this method.*
Give specific suggestions on how to improve the manuscript	*Your introduction needs more detail. I suggest that you improve the description at lines 57- 86 to provide more justification for your study (specifically, you should expand upon the knowledge gap being filled).*
Comment on language and grammar issues	*The English language should be improved to ensure that your international audience can clearly understand your text. I suggest that you have a native English speaking colleague review your manuscript. Some examples where the language could be improved include lines 23, 77, 121, 128 – the current phrasing makes comprehension difficult.*
Organize by importance of the issues, and number your points	*1. Your most important issue* *2. The next most important item* *3. …* *4. The least important points*
Give specific suggestions on how to improve the manuscript	*Line 56: Note that experimental data on sprawling animals needs to be updated. Line 66: Please consider exchanging "modern" with "cursorial".*
Please provide constructive criticism, and avoid personal opinions	*I thank you for providing the raw data, however your supplemental files need more descriptive metadata identifiers to be useful to future readers. Although your results are compelling, the data analysis should be improved in the following ways: AA, BB, CC*
Comment on strengths (as well as weaknesses) of the manuscript	*I commend the authors for their extensive data set, compiled over many years of detailed fieldwork. In addition, the manuscript is clearly written in professional, unambiguous language. If there is a weakness, it is in the statistical analysis (as I have noted above) which should be improved upon before Acceptance.*

Eocene Loranthaceae pollen revives the Gondwana breakup hypothesis for the family

Friðgeir Grímsson Corresp., [1] , **Paschalia Kapli** [2] , **Christa-Charlotte Hofmann** [1] , **Reinhard Zetter** [1] , **Guido W Grimm** Corresp. [1, 3]

[1] Department of Palaeontology, University of Vienna, Wien, Austria
[2] The Exelixis Lab, Scientific Computing Group, Heidelberg Institute for Theoretical Studies, Heidelberg, Germany
[3] None, Orléans, France

Corresponding Authors: Friðgeir Grímsson, Guido W Grimm
Email address: fridgeir.grimsson@univie.ac.at, grimmiges@gmail.com

Background. We revisit the palaeopalynological record of Loranthaceae, using pollen ornamentation to discriminate lineages and to test molecular dating estimates about the origin of aerial parasitism in this Santalales family.

Methods: Fossil Loranthaceae pollen from the Eocene and Oligocene are analysed and documented using scanning-electron microscopy. These fossils were associated with molecular-defined clades and used as minimum age constraints for Bayesian node dating using different topological scenarios.

Results: The fossil Loranthaceae pollen document the presence of at least one extant root-parasitic lineage (Nuytsieae) and two aerial parasitic lineages (Psittacanthinae and Loranthinae) by the end of the Eocene in the Northern Hemisphere. If the modern situation reflects the one in the past, aerial parasitism in Loranthaceae evolved much earlier than previously suggested and possibly multiple times. All currently available data point to the late Cretaceous-Paleogene continental breakup as the main trigger for initial diversification in Loranthaceae.

Discussion: With the generation of molecular data becoming easier and cheaper every day, neontological research should re-focus on conserved morphologies that can be traced in the fossil record. The pollen, representing the male gametophytic generation of plants and often a taxonomic indicator, can be such a tracer. Analogously, palaeontological research should put more effort in diagnosing Cenozoic fossils with the aim of including them into modern-systematic frameworks.

Eocene Loranthaceae pollen revives the Gondwana breakup hypothesis for the family

Friðgeir Grímsson[1], Pashalia Kapli[2], Christa-Charlotte Hofmann[1], Reinhard Zetter[1], Guido W. Grimm[1,3]

[1] University of Vienna, Department of Palaeontology, Vienna, Austria

[2] The Exelixis Lab, Scientific Computing Group, Heidelberg Institute for Theoretical Studies, Heidelberg,

[3] Unaffiliated, Orléans, France

Corresponding Authors:

Friðgeir Grímsson: fridgeir.grimsson@univie.ac.at

Guido Grimm: grimmiges@gmail.com

Introduction

The Loranthaceae (order Santalales), a moderately large family comprising about 76 genera and over 1000 species in five tribes (Nickrent 1997 onwards; Nickrent et al. 2010), has a wide geographical distribution. Today, there is a relatively clear geographic split between a New World group (Psittacanthinae) and Old World-Australasian lineages (Elythrantheae and Lorantheae), which gave rise to the hypothesis that the initial Loranthaceae diversification was linked to the final phase of the Gondwana breakup in the Late Cretaceous (e.g. Barlow 1990; Vidal-Russell & Nickrent 2007). Only three of the more than 70 genera are root parasites and the rest are aerial branch parasites. Molecular studies on Loranthaceae (and Santalales in general) have thus focused on three issues: 1) to clarify the evolutionary relationships within the family (Vidal-Russell & Nickrent 2008a); 2) to explain the transition from root to aerial parasitism (Wilson & Calvin 2006); 3) to date the time of transition to aerial parasitism (Vidal-Russell & Nickrent 2008b). All molecular studies using outgroups recognised the south-western Australian, root-parasitic monotypic *Nuytsia* R.Br. (monogeneric tribe Nuytsieae; Nickrent et al. 2010) as the first diverging lineage in the family (Wilson & Calvin 2006; Vidal-Russell & Nickrent 2008a; Su et al. 2015). The other two Loranthaceae root parasites (*Atkinsonia* F.Muell., *Gaiadendron* G.Don; tribe Gaiadendreae) formed a grade to the New World aerial parasites (Wilson & Calvin 2006; multiple origins of aerial parasitism) or all aerial parasitic genera of the family (Vidal-Russell & Nickrent 2008a; Vidal-Russell & Nickrent 2008b; Su et al. 2015; singular origin). Using a time-calibrated phylogeny, Vidal-Russell and Nickrent (2008b) concluded that Loranthaceae diverged from other Santalales lineages in the uppermost Cretaceous. First radiation – divergence of root parasites *Nuytsia*, *Atkinsonia* and *Gaiadendron* – was during the Eocene. The crown age of the aerial parasitism clade within the Loranthaceae, comprising the mostly New World Psittacantheae and Old World-Australasian Erytrantheae and Lorantheae, was placed in the middle Oligocene, approximately 28 Ma; a time characterised by global cooling (Zachos et al. 2001) and retreat of subtropical and tropical vegetation.

Although molecular and morphological interrelationships of Loranthaceae genera are considered now to be relatively clear (Nickrent et al. 2010; Su et al. 2015; but see Grímsson, Grimm & Zetter 2017), the timing of divergence between the genera has not been compared to available evidence from the fossil record (e.g. Muller 1981; Song, Wang & Huang 2004; Macphail et al. 2012). Also, the phytogeographic history of the family is based merely on the

present distribution of its genera (e.g. Vidal-Russell & Nickrent 2007) and has not yet been explored in detail (Vidal-Russell & Nickrent 2008a: p. 1027). The latest hypothesis put forward was that Loranthaceae originated when South America, Antarctica and Australia were still connected, and that two large-scale migration events, one from New Zealand and one from Australia shaped the modern distribution (Vidal-Russell & Nickrent 2008a, 2008b). Since evolution of aerial parasitism was estimated to be of middle Oligocene age, older fossil records, the oldest going back to the early Eocene (c. 50 Ma) in Australia, were considered to represent root parasites or extinct clades of aerial parasites (Macphail et al. 2012).

The outstanding work on the pollen morphology of extant Loranthaceae by Feuer & Kuijt (1979, 1980, 1985) and other Santalales lineages (Maguire, Wurdack & Huang 1974; Feuer 1977, 1978, 1981; Feuer & Kuijt 1978, 1982; Feuer, Kuijt & Wiens 1982) demonstrated that most pollen produced by members of the Loranthaceae cannot be confused with pollen from other angiosperm families (Grímsson, Grimm & Zetter 2017). Grímsson, Grimm & Zetter (2017) distinguished four general types (Pollen Type A, B, C, D), of which only one (Pollen Type A) could be confused with pollen of other Santalales lineages and would unlikely be recognised as Loranthaceae pollen if found in a fossil pollen sample. Combined application of light microscopy (LM), scanning-electron microscopy (SEM), and transmission electron microscopy (TEM) revealed that pollen morphologies—including the many variants of B-type pollen—are further conserved at various taxonomic levels, from certain genera to tribes, within Loranthaceae (Feuer & Kuijt 1978, 1979, 1980; Feuer & Kuijt 1985; Caires 2012; Grímsson, Grimm & Zetter 2017). Thus, dispersed fossil pollen can aid in the reconstruction of past distribution of Loranthaceae lineages and shed light on the timing of the origin of the modern aerial parasitic clades.

Here, we describe new fossil Loranthaceae pollen grains from the middle Eocene of the United States, Greenland, Central Europe, and East Asia, and from the late Oligocene/early Miocene of Germany. The diagnostic morphological features of the pollen provided sufficient details to assign the fossil pollen to distinct lineages within the Loranthaceae. These fossil pollen represent the earliest unambiguous reports of the root parasitic Nuytsieae, and the (today) aerial parasitic lineages Psittacanthinae, Elytrantheae and Lorantheae. Thus, they can be used as potential ingroup minimum age priors for node dating and to refine our knowledge about the biogeographic history of the Loranthaceae.

Material & Methods

Origin of samples and geological background (Table 1)

The fossil Loranthaceae pollen identified during this study occurred in six different sediment samples: (1) the Claiborne Group of the Miller Clay Pit in Henry County, Tennessee, United States (sample UF 15817-062117); (2) the Hareøen Formation (middle Eocene) on Qeqertarsuatsiaq Island (Hareøen), western Greenland; (3) the Borkener coal measures of the Stolzenbach underground coal mine, near Kassel, Germany; (4) the Profen Formation (middle Eocene) of the Profen opencast mine, close to Leipzig in Germany; (5) the Changchang Formation (middle Eocene) on northern Hainan Island, South China; (6) the Melker Series of the NÖ05 borehole positioned close to Theis, near Krems, Lower Austria; and (7) the Cottbus/Spremberg Formations (late Oligocene/early Miocene) of Altmittweida in Saxony, Germany. For details on the geographic positions, geology, paleoecology, and previously known fossil plants from these formations and localities see Table 1 and references therein.

Preparation of samples

The sedimentary rock samples were processed according to the protocols outlined in Grímsson, Denk & Zetter (2008). We investigated the fossil Loranthaceae pollen grains using the 'single grain method' (Zetter 1989), whereby the same fossil pollen grain is first analysed under the LM and then SEM. SEM stubs produced under this study are stored in the collection of the Department of Palaeontology, University of Vienna, Austria, under accession numbers IPUW 7513/076-100.

Molecular framework (File S1: Steps 1–3 of analysis pipeline)

For molecular data we relied on a 2014 NCBI GenBank harvest compiled for an earlier study (Grímsson, Grimm & Zetter 2017). Gene banks now (per Dec 1st, 2016) include ~100 additional accessions (File S2); but the majority of these are either microsatellite marker sequences or sequences of gene regions too variable, or with insufficient taxonomic coverage within the Loranthaceae, to be of any use; thus, we opted against updating dataset harvested for the preceding study.

Given the problems with signals in Loranthaceae sequence data (Grímsson, Grimm & Zetter 2017, files S1, S6), we used the following protocol to prepare data sets for phylogenetic inferences and molecular dating (a detailed description is provided in File S1). First (step 1) we performed single-gene maximum likelihood (ML) inferences for five candidate gene regions using the complete harvested data with RAxML v. 8.2.4 (Stamatakis 2014). This was mainly done to cross-check for problematic accessions and to test the phylogenetic coherence of multiple accessions of the same species/genus. As consequence, we eliminated several more sequences, in addition to the ones not considered earlier, for computing strict genus-consensus sequences (see File S1, an emended version of Grímsson, Grimm & Zetter 2017, file S2). The second step was to consense and concatenate the unproblematic data: strict species-consensus sequences, i.e. sequences summarising the information of accessions attributed to a species, were computed with G2CEF (Göker & Grimm 2008) and concatenated with MESQUITE v. 2.75 (Maddison & Maddison 2011). The third and final step was the inference of single- and oligo-gene ML trees using RAxML v. 8.2.4; branch support was established using non-parametric bootstrapping with the number of necessary bootstrap replicates determined by the extended majority rule consensus bootstop criterion (Pattengale et al. 2009). Potentially conflicting signal was explored using bootstrap (BS) consensus networks (bipartition networks; Grimm et al. 2006), a special form of consensus networks (Holland & Moulton 2003) generated with SPLITSTREE v. 14.2 (option "count", Huson & Bryant 2006) in which edge length are proportional to the frequency of the according split in the BS (pseudo)replicate sample.

Clock-rooting (Table 2; Step 4 of analysis pipeline)

A recent re-analysis of available molecular data using genus-consensus sequences (Grímsson, Grimm & Zetter 2017) failed to unambiguously resolve basal relationships in Loranthaceae as was the case in earlier studies using placeholder accessions (Wilson & Calvin 2006; Vidal-Russell & Nickrent 2008a; Su et al. 2015; see Grímsson, Grimm & Zetter 2017, file S6, for a critical assessment of the Loranthaceae data included by Su et al.). The problem of topological ambiguity worsens for the species tree inferred here, in part due to data gaps (see *Inferences*). Due to issues regarding ambiguity of the deepest splits within the Loranthaceae and likely outgroup-ingroup long-branch attraction (Grímsson, Grimm & Zetter 2017, file S6), we inferred an alternative, clock-based root (Huelsenbeck, Bollback & Levine 2002) for the Loranthaceae

tree using BEAST (Drummond & Rambaut 2007; Drummond et al. 2012), following the example of an earlier study on *Acer* (Renner et al. 2008). Clock-rooting was performed for five main datasets differing in the gene region coverage (all gene regions, all but excluding the most variable *trn*L-*trn*F spacer region, only plastid regions including or excluding the *trn*L-*trn*F spacer, only nuclear regions). In addition, the taxon-reduced data set used for the final dating step was analysed (for further details see File S1).

Basic setup of molecular dating (Table 2; Steps 5 and 6 of analysis pipeline)

Nine of the 13 new described fossil pollen from the Eocene to Oligocene (see **Results**) were used as minimum age constraints (informing 3–5 node height priors per analysis) for traditional node dating using a Bayesian uncorrelated clock (UC) approach; analyses were performed with BEAST v. 1.8.2. Table 2 lists the age priors used for the analyses. Dating was done in two phases (for set-up details see File S1).

In the initial phase (Step 5), we inferred dated species phylogenies based on the complete concatenated data set for three rooting scenarios: *(i)* the commonly accepted root placing *Nuytsia* as sister to all other Loranthaceae (Vidal-Russell & Nickrent 2008a; Nickrent et al. 2010; Su et al. 2015); *(ii)* a clock-inferred root recognising the predominately Old World Lorantheae as sister to a mainly southern hemispheric clade including all three root parasites, the Psittancantheae and Elytrantheae (see *Results*); and *(iii)* recognising *Tupeia* as sister to all other Loranthaceae. The 3rd scenario is based on the hypothesis that the typical oblate, ± triangular Loranthaceae pollen (Pollen Type B in Grímsson, Grimm & Zetter 2017, a pollen type unique within the Santalales) evolved only once. The monotypic *Tupeia* is one of two Loranthaceae species with a spheroidal, echinate pollen as found in other Santalales lineages (Grímsson, Grimm & Zetter 2017) and the only one sequenced so far.

For the final dating (Step 6), we used a taxon-reduced data set limited to 42 species covering all included gene regions to counter problems with missing data in the full data set. At this step we also included an alternative topology, constraining the primary branching patterns as seen in the tree of Su et al. (2015), which depicts the "correct relationships" between the major lineages and potentially early diverging, isolated, monotypic genera (Anonymous, pers. comm., 2016)

Descriptions (Figs 1–6)

Some lineages (tribes, subtribes) and genera of modern Loranthaceae are characterised by unique pollen morphologies (autapomorphies in a strict Hennigian sense) or specific pollen character suites (Grímsson, Grimm & Zetter 2017). Nevertheless, we refrained from using genus names to address the fossil pollen types described here – even if the pollen is highly similar to indistinguishable from a modern counterpart – for several reasons: (1) intra- and interspecific variation is not comprehensively understood in Loranthaceae; (2) the generic concepts in Loranthaceae are under on-going revision, (3) monotypic modern lineages/genera could have been more widespread and diverse in the past; and (4) occurrence of fossils combining features of two or more genera or lineages. Thus, all pollen grains are classified as morphotypes (MT) named after the locality, where they were found.

All fossil pollen described here falls within the variation of Pollen Type B according Grímsson, Grimm & Zetter (2017). Pollen grains of Type B are oblate (to various degrees), triangular to trilobate in polar view and show a ± psilate sculpturing in LM. They are basically syn(3)colpate, but also demisyn(3)colpate and zono(3)colpate in some genera/lineages. Usually, no further sculpturing details can be observed in LM except for occasional exine thickening or thinning at the pole (e.g. Fig. 1C, H, M, Y) and along the colpi or in the mesocolpium (e.g. Fig. 1C, D, R).

Miller Clay Pit MT1, aff. Nuytsia *(Figs 1A, 1B, 2A, SH; Plate S01, S02 in File S3)*

Description—Pollen, oblate, concave triangular in polar view, no undistorted equatorial view available, equatorial apices obcordate, interapertural areas (mesocolpia) sunken; pollen small, equatorial diameter 15.0–18.3 µm in LM, 13.0–14.4 µm in SEM; zono(3)colpate, colpi long and narrow; exine 0.7–0.8 µm thick, nexine thinner than sexine; tectate; sculpturing psilate in LM, microechinate in area of mesocolpium in SEM, echini 0.3–0.8 µm long, 0.2–0.5 µm wide at base (SEM); margo well developed, broad, psilate to partly granulate (SEM); colpus membrane not observed.

Locality—Miller Clay Pit, Henry County, Tennessee, United States (Table 1).

Remarks—This pollen type is very similar to pollen of the extant southwestern Australian *Nuytsia floribunda* (Labill.) G.Don as figured by Feuer & Kuijt (1980) and Grímsson, Grimm & Zetter (2017); a pollen readily distinct from all other modern Loranthaceae. The fossil pollen only differs from *Nuytsia* by being zonocolpate and showing sunken (infolded) mesocolpia in LM and SEM. The shift from the basic syncolpate organisation to zonocolpate can be observed in several lineages of (modern) Loranthaceae. With respect to the high genetic distinctness of *Nuytsia* from all other Loranthaceae, the modern species likely represents the sole survivor of an early diverged lineage of root parasitic loranths. Hence, it is likely that ancestral or extinct members of *Nuytsia*/Nuytsieae had more morphological variation than can be observed in the sole surviving species.

Use as age constraint—The Miller Clay Pit MT1 can be used to constrain the root age of the lineage leading to *Nuytsia*, i.e. the Nuytsieae root age. Based on the currently available data, the relationship of *Nuytsia* to the remainder of the genus and the other two extant root parasites is unclear. Nevertheless, it is clear that *Nuytsia* is the sole modern-day representative of an early diverging lineage. For rooting scenario 1 (outgroup-inferred root) Miller Clay Pit MT1 serves as minimum age constraint for the MRCA of all (extant) Loranthaceae.

Miller Clay Pit MT2, aff.* Tripodanthus *(Figs 1C, 3A, 3G; Plate S03 in File S3)

Description—Pollen, oblate, concave-triangular in polar view, no undistorted equatorial view available, equatorial apices T-shaped; pollen small, equatorial diameter 18.3–21.7 µm in LM, 17.9–20.2 µm in SEM; syn(3)colpate, colpi narrow; exine 1.2–1.5 µm thick, nexine thinner than sexine, intercolpial nexine thickening at pole, sexine thickened in area of mesocolpium (LM); tectate; sculpturing psilate in LM, (micro)baculate in area of mesocolpium in SEM, (micro)bacula densely packet, 0.2–0.9 µm long, 0.2–0.4 µm wide (SEM); margo well-developed, widening towards pole and equator, mostly psilate, with few nanoechini/-verrucae (SEM); colpus membrane not observed.

Locality—Miller Clay Pit, Henry County, Tennessee, United States (Table 1).

Remarks—Pollen grains of this morphotype show the exclusive morphology of pollen of two of the three extant *Tripodanthus* species*: T. acutifolius* (Ruiz & Pav.) Tiegh. and *T. flagellaris* Tiegh. as described and figured by Feuer & Kuijt (1980) and Grímsson, Grimm & Zetter (2017).

The recently described *T. belmirensis* F.J.Roldán & Kuijt has a different, more compact type of pollen (Roldán & Kuijt 2005). All species are endemic to South America (e.g., Amico et al. 2012).

Use as age constraint—Representing a characteristic pollen type known only from two modern species of the same genus, Miller Clay Pit MT2, MT3, and the Aamaruutissaa MT could be used as minimum age constraints for the MRCA of *Tripodanthus* with respect to *T. belmirensis* and its different pollen. We followed a more conservative approach here. *Tripodanthus* is often reconstructed as the first diverging branch within the Psittacanthinae, followed in most trees by *Psittacanthus.* The latter is a genus with diverse pollen (Feuer & Kuijt 1979), including morphologies more similar to those of *Tripodanthus* and its fossil counterparts than to the remainder of the subtribe (and *T. belmirensis*), characterised by compact B-type pollen with minute to indistinct sculpturing and pollen grains of the Type C (*Passovia pyrifolia, Dendropemon*) and D (*Oryctanthus*). Compact B-type, C-type and D-type pollen occur much later in the fossil record (File S4) and are completely missing in our samples. The latter three types appear to be derived. Taken all evidence together, we cannot exclude the possibility that *Tripodanthus acutifolius* and *T. flagellaris* simply retained an (more) ancestral pollen type of the Psittacanthinae. The fossil pollen grains hence would not indicate the presence of the genus *Tripodanthus* in North America and Greenland*,* but of extinct, northern-hemispheric or ancestral members of the Psittacanthinae and informing a conservative minimum age for the MRCA of Psittacanthinae and their sister clade. Unfortunately, this sister clade, if not constrained (scenario 4), is not resolved with meaningful support. As a trade-off, we used the Aamaruutissaa MT—the most precisely dated pollen of the *Tripodanthus*-like MTs and likely younger than their American counterparts—as minimum age constraint for the MRCA of the Psittacanthinae lineage for the rooting scenarios 1–3 under the assumption that crown radiation within the Psittacanthinae must have started before the time a loranth producing *Tripodanthus*-like pollen thrived in Greenland, far outside the modern distribution area of the family.

Miller Clay Pit MT3, aff. **Tripodanthus** ***(Figs 1D, 3B, 3C, 3H, 3I; Plate S04 in File S3)***

Description—Pollen, oblate, slightly concave-triangular in polar view, no undistorted equatorial view available, equatorial apices truncated; pollen small, equatorial diameter 20.0–21.7 µm in LM, 19.6–21.3 µm in SEM; syn(3)colpate, colpi narrow; exine 0.9–1.6 µm thick, nexine thinner than sexine, intercolpial nexine thickening at pole, sexine thickened in area of mesocolpium (LM); tectate; sculpturing psilate in LM, (micro)baculate and perforate in area of mesocolpium in SEM, (micro)bacula densely packet, (micro)bacula 0.4–1.8 µm long, 0.1–0.2 µm wide; margo well developed, markedly broader in equatorial regions, margo faintly nano- to microrugulate (SEM); colpus membrane nanoverrucate to granulate (SEM).

Locality—Miller Clay Pit, Henry County, Tennessee, United States (Table 1).

Remarks—General outline and size of the Miller Clay Pit MT3 is very similar to those of Miller Clay Pit MT2. The main difference is that the margo in Miller Clay Pit MT3 can be faintly rugulate, a feature not observed in Miller Clay Pit MT2 or the two modern species with nearly identical pollen. Also, the mesocolpium is perforate in Miller Clay Pit MT3; a feature not seen in Miller Clay Pit MT2 or extant *Tripodanthus*. As a trend, the sculptural elements are narrower and can be much longer than in Miller Clay Pit MT2 pollen.

Use as age constraint—See Miller Clay Pit MT2.

Aamaruutissaa MT, aff. **Tripodanthus** ***(Figs 1E, 3D, 3J; Plate S05 in File S3)***

Description—Pollen, oblate, slightly concave-triangular in polar view, no undistorted equatorial view available, equatorial apices truncated; pollen small, equatorial diameter 18.6–22.0 µm in LM, 18.5–21.5 µm in SEM; syn(3)colpate; exine 1.0–1.3 µm thick, nexine thinner than sexine, intercolpial nexine thickening at pole (LM); tectate; sculpturing psilate in LM, nano- to microbaculate in area of mesocolpium in SEM, bacula 0.3–1.1 µm long, 0.2–0.3 µm wide (SEM); margo well developed, margo faintly nano- to microrugulate (SEM); colpus membrane nanoverrucate to granulate (SEM).

Locality—Aamaruutissaa, southeast Qeqertarsuatsiaq Island, western Greenland (Table 1).

Remarks—This pollen type has previously been figured as Loranthaceae gen. et spec. indet. (Manchester, Grímsson & Zetter 2015, fig. 2A–C). Like Miller Clay Pit MT2 and MT3, it is nearly indistinguishable from the pollen of the two original species of *Tripodanthus, T.*

acutifolius and *T. flagellaris*. The Aamaruutissaa MT pollen combines the mesocolpial sculpturing seen in Miller Clay Pit MT2 with the shape and margo seen in Miller Clay Pit MT3. With respect to the modern species, both the Tennessee (Miller Clay Pit MT2, MT3) and Greenland pollen grains (Aamaruutissaa MT) were possibly produced by the same genus or at least closely related taxa of the same loranth lineage (Psittacanthinae).

Use as age constraint—See Miller Clay Pit MT2.

Stolzenbach MT, pollen of ambiguous affinity (Figs 1F, 2B, 2I; Plate S06 in File S3)

Description—Pollen, oblate, trilobate in polar view, no undistorted equatorial view available, equatorial apices obcordate, interapertural areas (mesocolpia) sunken; pollen small, equatorial diameter 12.1–15.4 µm in LM, 11.7–15.3 µm in SEM; syn(3)colpate, colpi narrow; exine 0.7–0.9 µm thick, nexine thinner than sexine; tectate; sculpturing psilate in LM, microechinate in area of mesocolpium in SEM, echini stout with blunt apices, 0.4–0.8 µm long, 0.3–0.8 µm wide at base (SEM); margo well developed, broad, covering the grain's surface in polar view, microrugulate, granulate (SEM); colpus membrane mostly granulate (SEM).

Locality—Stolzenbach underground coalmine, Kassel, Germany (Table 1).

Remarks—Size, outline, and form of the pollen, and SEM sculpturing in the area of the mesocolpium is most similar to what has been observed in pollen of modern monotypic root-parasites *Nuytsia* and *Gaiadendron*, and the Lorantheae *Muellerina* (Ileostylinae). Despite this general similarity, the pollen differs from the modern ones and pollen with affinity to *Nuytsia* reported from the Miller Clay Pit, Tennessee (Miller Clay Pit MT1), visually (compare overviews in Fig. 2B, E, F, G) and regarding its sculpturing. The Stolzenbach MT echini are sparsely packed and broader at the base; the striae on the margo are flatter and broader. The pollen may well represent an (unrelated) extinct lineage or ancestral taxon with affinities to both the root-parasitic lineages and/or the Lorantheae.

Use as age constraint—Although the pollen cannot be assigned to any modern genus or lineage, it is an early Central European representative of the common Pollen Type B of Loranthaceae. Its morphology is in many aspects primitive within the (B-type) Loranthaceae, hence, the similarity with *Nuytsia*/Miller Clay Pit MT1, *Gaiadendron* and *Muellerina* (the only Lorantheae known so far with a striate ornamentation). Its morphology, place, and age would fit

for an early precursor or extinct sister lineage of the Lorantheae. Taken together with the coeval pollen from North America and Greenland, it provides evidence for the onset of diversification of B-type pollen lineages including the possible establishment of the Lorantheae. Hence, it was used to constrain the minimum age of the MRCA of all Loranthaceae (rooting scenario 2; clock-based root) or Loranthaceae with B-type pollen (rooting scenario 3; pollen morphology-informed root).

Profen MT1, pollen of unknown affinity (Figs 1G, 1H, 2C, 2J; Plate S07 in File S3)

Description—Pollen, oblate, trilobate in polar view, elliptic in equatorial view, lobes very narrow, equatorial apices obcordate, interapertural areas (mesocolpia) sunken; pollen small, polar axis 10.0-12.3 µm long in LM, 9.5–11.0 µm long in SEM, equatorial diameter 13.8–17.5 µm in LM, 11.9–13.8 µm in SEM; syn(3)colpate; exine 0.9–1.1 µm thick, nexine thinner than sexine; tectate; sculpturing psilate in LM, nanoechinate, nanobaculate, granulate in area of mesocolpium in SEM, echini/bacula 0.3–0.6 mm long, 0.2–0.4 µm wide (SEM); margo well-developed, covering nearly the entire surface of the grain in polar view, faintly microrugulate (SEM); colpus membrane nanoverrucate to granulate (SEM).

Locality— Profen, Leipzig, Central Germany (Table 1).

Remarks—Like the Stolzenbach MT pollen this fossil pollen type has no direct modern counterpart. These small, narrow-lobate pollen grains with their finely sculptured, deeply sunken mesocolpia characteristic of the Profen MT1 pollen are not found in any modern taxon, but bear some similarity to the younger (Oligocene) pollen of Theiss (see later). Equally small pollen grains are only known from the root-parasites *Nuytsia* and *Gaiadendron*, and the Lorantheae *Muellerina*. Equally minute sculpturing is only found in otherwise completely different, and putatively derived pollen of deeply nested (phylogenetically) Psittacanthinae and Lorantheae.

Use as age constraint—Showing a unique combination of putatively primitive and derived morphological features, this pollen could only be used to constrain the minimum age of the MRCA of all Loranthaceae with B-type pollen.

Profen MT2, aff.* Notanthera *(Figs 1I, 1J, 4A, 4B, 5A, 5B; Plate S08 in File S3)

Description—Pollen, oblate, straight- to slightly concave-triangular in polar view, no undistorted equatorial view available, equatorial apices obcordate; pollen small, equatorial diameter 21.5–23.1 µm in LM, 18.3–19.6 µm in SEM; syn(3)colpate, colpi narrow; exine 1.1–1.4 µm thick, nexine thinner than sexine, intercolpial nexine thickening at pole, sexine thickened in area of mesocolpium (LM); tectate; sculpturing psilate in LM, nanoechinate/-baculate, perforate in area of mesocolpium in SEM, echini/bacula stout, sometimes fused, 0.2–0.4 µm long, 0.2–0.4 µm wide (SEM); margo well-developed, slightly widening towards pole and equator, psilate to faintly microrugulate (SEM); colpus membrane nanoverrucate to granulate (SEM).

Locality—Profen, Leipzig, Central Germany (Table 1).

Remarks—Form and sculpturing of pollen grains of this morphotype are remarkably similar to those of *Notanthera heterophylla* (Feuer & Kuijt 1980, fig. 5). *Notanthera heterophylla* is of two species included in the two monotypic genera that comprise the South American Notantherinae, a subtribe of the Psittacantheae neither resolved as clade nor rejected with high support in molecular-phylogenetic inferences (Grímsson, Grimm & Zetter 2017, files S1, S6). The sculpturing of Profen MT2 is furthermore in line with the description and TEM image provided by Feuer & Kuijt (1980).

Systematic note—The second species included in the Notantherinae, *Desmaria mutabilis* (Poepp. & Endl.) Tiegh. ex B.D.Jacks, has not only a different pollen (Feuer & Kuijt 1980; Grímsson, Grimm & Zetter 2017) but is also genetically distinct (Fig. 7).

Use as age constraint—This pollen can inform the minimum root age for the lineage leading to *Notanthera*, i.e. the minimum age of the MRCA of *Notanthera* and Elytrantheae (scenarios 1–3; preferred topology based on the taxon-reduced data set) or *Notanthera* and Psittacanthinae (scenario 4; topology constrained to fit with Su et al. 2015, fig. 1B).

Profen MT3, pollen of the Elytrantheae clade (Figs 1K, 4C, 5C; Plate S09 in File S3)

Description—Pollen, oblate, convex-triangular in polar view, no undistorted equatorial view available, equatorial apices more or less truncated; pollen small, equatorial diameter 20.0–21.5 µm wide in LM, 19.2–20.0 µm wide in SEM; syn(3)colpate, colpi very narrow at equatorial

apices, widening towards the pole; exine 0.9–1.1 µm thick, nexine thinner than sexine (LM); tectate; sculpturing psilate in LM, mostly nanobaculate to -echinate in area of mesocolpium in SEM, bacula/echini 0.2–0.5 µm long, 0.1–0.2 mm wide (SEM); margo well developed, covering the equatorial apices, mostly psilate, with few nanobacula/-echini in polar area, forming triangular protrusions at pole (SEM); colpus membrane nanoechinate/-verrucate to granulate (SEM).

Locality—Profen, Leipzig, Central Germany (Table 1).

Remarks—The combination of characters (syncolpate with widening colpi, margo with triangular protrusions and sculpturing reminiscent of the mesocolpium in polar area, sculpturing of mesocolpium nanobaculate/-echinate) is today only found in members of the Elytrantheae. With respect to studied modern Elytrantheae, the pollen of Profen MT3 is most similar to that of *Peraxilla tetrapetala* (Fig. 4), but the sculpturing elements are more slender and higher (Fig. 5). The sculpturing in the mesocolpium (dimension and density of sculptural elements) is very similar to grains included in another morphotype found at Profen (Profen MT4; Fig. 5).

Use as age constraint—Here we used Profen MT3, MT4 and MT5 to constrain the root age of the Elytrantheae, i.e. the minimum age of the MRCA of *Notanthera* and Elytrantheae (scenarios 1–3). Further studies of modern pollen of Elytrantheae at and below the genus level and more genetic data are needed to decide whether the Profen MT3, and the related Profen MT4 and MT5, are already indicative for a first divergence within the Elytrantheae and can be placed more decisively within the Elytrantheae subtree.

Profen MT4, possible pollen of the Elytrantheae clade (Figs 1L–O, 4D, 4E, 5D; Plate S10, S11 in File S3)

Description—Pollen, oblate, concave-triangular to trilobate in polar view, no undistorted equatorial view available, equatorial apices T-shaped; pollen small, polar axis 11.3–15.0 µm long in LM, equatorial diameter 17.5–25.0 µm wide in LM, 14.3–20.0 µm wide in SEM; demisyn(3)colpate, colpi short (SEM), widening towards the pole forming a polar depression (polar sexine reduced); exine 1.1–1.3 µm thick, nexine thinner than sexine, nexine hexagonally thickened in polar area (LM); tectate; sculpturing psilate in LM, mostly nanobaculate/-echinate in SEM, bacula/echini 0.3–1.1 µm long, 0.1–0.4 µm wide at base (SEM); margo indistinct in

polar area, more prominent in equatorial regions, faintly microrugulate, covered by nanobacula/-echini in polar area (SEM); colpus membrane nanoechinate/-verrucate to granulate (SEM).

Locality—Profen, Leipzig, Central Germany (Table 1).

Remarks— This pollen type has previously been figured as Loranthaceae gen. et spec. indet. (Manchester, Grímsson & Zetter 2015, fig. 2D–F). Sculpturing of Profen MT4 is somewhat variable, dimensions, density and shape of sculptural elements resemble those in Profen MT3 and Profen MT5 (see later), or are overlapping between both. Regarding its form (trilobate with T-shaped equatorial apices) and lacking a distinct margo in the polar area, the pollen differs from all modern members of the Elytrantheae. In this aspect, it is similar to the pollen of *Ligaria* (Psittacantheae: Ligarinae), a genus with ambiguous phylogenetic affinities to other New World genera (Grímsson, Grimm & Zetter 2017, file S1, figs S6-1–9). Also in *Ligaria*, the sexine is reduced in the polar area (Fig. 4), the generally very narrow colpi are fusing in a triangular polar depression (a feature only seen in *Ligaria* and its putative relative *Tristerix*). *Ligaria* pollen grains are furthermore distinctly microbaculate (Fig. 5). Bacula are found in all three Profen morphotypes linked to the Elytrantheae lineage, but are rare or absent in the modern members of this clade.

Use as age constraint—See Profen MT3.

Profen MT5, probable pollen of the Elytrantheae clade (Figs 1P, 1Q, 4F, 5E; Plate S12 in File S3)

Description—Pollen, oblate, straight-triangular in polar view, elliptic to subrhombic in equatorial view, equatorial apices broadly rounded; pollen small to medium, polar axis 7.5–11.5 µm long in LM, equatorial diameter 21.5–30.0 µm wide in LM, 18.7–24.4 µm wide in SEM; demisyn(3)colpate, widening towards pole, terminating halfway between pole and equator (SEM); exine 1.1–1.3 µm thick, nexine thinner than sexine (LM); tectate; sculpturing psilate in LM, mostly nano- to microbaculate/-echinate in area of mesocolpium in SEM, bacula/echini 0.3–0.7 µm long, 0.1–0.3 mm wide at base; margo distinct but not raised, mostly psilate, with few nanobacula/-echini in polar area, forming triangular protrusions at pole (SEM); colpus membrane nanoechinate/-verrucate to granulate (SEM).

Locality—Profen, Leipzig, Central Germany (Table 1).

Remarks— The pollen fits with the morphotypes seen in modern members of the Elytrantheae, although its combination of characters is unique. Small, demisyncolpate, (sub)rhombic pollen grains are (so far) only known from *Amylotheca*, which differ from the fossil pollen by their outline in polar view (Fig. 4) and sculpturing (Fig. 5). Regarding the latter, Profen MT5 is very similar to grains included in Profen MT3. Both, Profen MT3 and MT5, differ from the third morphotype with possible affinities to Elytrantheae (Profen MT4) by their demisyncolpate grains (Fig. 4). Regarding the mesocolpium, Profen MT5 shows the densest sculptured mesocolpium of all three morphotypes (Fig. 5).

Use as age constraint—See Profen MT3.

Changchang MT, aff. Amyeminae vel Scurrulinae (Figs 1R, 1S, 6A, 6B, 6H, 6I; Plate S13 in File S3)

Description—Pollen, oblate, concave-triangular to broadly trilobate in polar view, no undistorted equatorial view available, equatorial apices broadly rounded; pollen small, equatorial diameter 21.1–24.4 µm wide in LM, 19.1–21.8 µm wide in SEM; syn(3)colpate; exine 0.9–1.1 µm thick, nexine thinner than sexine; tectate; sculpturing psilate in LM, nanoverrucate to granulate, perforate in SEM, granula partly fused; margo well developed, psilate, widening towards the equator, usually covering the entire apex (SEM); colpus membrane granulate; rhombic structures (opercula) covering equatorial apices (SEM).

Locality—Changchang Basin, Jiazi Town, northern Hainan Island (Table 1).

Remarks—The minute sculpturing and its basic form link this pollen to the Lorantheae, in particular to the Scurrulinae *Taxillus* and *Scurrula* (unresolved within Clade J) on one hand, and *Amyema* (Amyeminae; Clade I in Vidal-Russell & Nickrent 2008a, sister clade of Clade J) on the other hand. The pollen could be described as a Scurrulinae pollen with an *Amyema*-like margo. A unique feature not found in any modern Loranthaceae so far are the operculum-like triangular structures of the equatorial apices. Pollen of the two first diverging, long-branched lineages in Lorantheae (Clades G and H in Vidal-Russell & Nickrent 2008a; cf. Su et al. 2015, figs 1B, S7; Grímsson, Grimm & Zetter 2017, fig. 2) are markedly distinct. Thus, we think that this pollen either belongs to an extinct or ancestral Lorantheae lineage related to the core Lorantheae (= Clades I and J according Vidal-Russell & Nickrent).

Use as age constraint—Based on its morphology, the Changchang MT could already represent an early member of the Lorantheae core clade, i.e. would inform a minimum age of the MRCA of Lorantheae core clade and its sisterclade Ileostylinae. However, some molecular data sets indicate a sister relationship between Ileostylinae and Loranthinae (cf. Grímsson, Grimm & Zetter 2017, files S1, S6). Furthermore, more information on pollen morphology in Lorantheae would be needed to exclude the possibility that the Changchang MT is correctly recognised as a representative of the Lorantheae core clade. Two of the four genera of the sister lineages of the core Lorantheae (Loranthinae, Ileostylinae) have not yet been studied palynologically and little is known on the other Amyeminae genera, the first diverging branch within the core Lorantheae. Hence, we opted for a more conservative approach and used the Changchang MT to constrain the MRCA of all Lorantheae.

Theiss MT (Figs 1T–X, 2D; Plate S14, S15 in File S3)

Description—Pollen, oblate, trilobate in polar view, emarginate in equatorial view, lobes very narrow, equatorial apices rounded; pollen small, polar axis 8.3-11.7 mm long in LM, 6.5-8.3 µm long in SEM, equatorial diameter 10.0–15.0 µm in LM, 10.3–11.8 µm in SEM; demisyn(3)colpate; exine 0.9–1.2 µm thick, nexine thinner than sexine (LM); tectate; sculpturing psilate in LM, nano- to microverrucate in area of mesocolpium in SEM, verrucae often fused, widely spaced, verrucae composed of conglomerate granula (SEM); margo well-developed, covering nearly the entire surface of the grain in polar view, faintly microrugulate, granulate (SEM); colpus membrane unknown.

Locality—Theiss, borehole southeast of Krems, Lower Austria (Table 1).

Remarks—This fossil pollen type has no direct modern counterpart. A unique feature are the widely spaced verrucae in area of mesocolpium. Demisyncolpate grains evolved at least three times in the Loranthaceae: in *Amylotheca* (Elytrantheae), in the *Cladocolea-Struthanthus* lineage and *Passovia* (Psittacanthinae), and *Tapinanthus* (*T. bangwenensis* [Engl. & K.Krause] Danser, *T. ogowensis* [Engl.] Danser; Lorantheae core clade). The fossil pollen shares no further feature with either Elytrantheae or Psittacanthinae. Grains with narrow (deflated) equatorial lobes, in which the margo extends beyond the mesocolpial plane, are so far only known from several members of the Lorantheae core clade (e.g. *Englerina, Globimetula, Phragmanthera*).

Mesocolpia with exclusively nanoverrucate to granulate sculpturing are only found in members of the Lorantheae. For instance, the Tapinanthinae (core Lorantheae) *Actinanthella* has emarginate, trilobate (to convex-triangular) pollen grains with a well-developed, mostly psilate margo and nanoverrucate to granulate mesocolpium, but they differ from the fossil pollen by their size and zonocolpate apertures.

Use as age constraint—With respect to its unique morphology and the yet superficial knowledge about pollen evolution in Lorantheae (see Changchang MT), we decided against using the Theiss MT to constrain a node higher up in the tree (e.g. the MRCA of Tapinanthinae and Emelianthinae) at this point.

Altmittweida MT, aff. **Helixanthera** ***(Figs 1Y–Ä, 6C, 6D, 6J; Plate S16 in File S3)***

Description—Pollen, oblate, convex-triangular in polar view, emarginate in polar view, equatorial apices broadly obcordate; pollen small, polar axis 4.4–5.5 µm long in LM, equatorial diameter 14.4–17.8 µm wide in LM, 13.7–16.0 µm wide in SEM; syn(3)colpate; exine 0.9–1.1 µm thick, nexine thinner than sexine, intercolpial nexine thickening at pole, sexine partly reduced in polar area (SEM); tectate; sculpturing psilate in LM, nano- to microverrucate, granulate in SEM, verrucae composed of conglomerate granula (Fig. 6J); margo psilate to microverrucate, granulate; colpus membrane nanoverrucate to granulate (SEM).

Locality—Altmittweida, Saxony, Germany (Table 1).

Remarks—This pollen type has previously been be figured by Kmenta (2011, plate 11, figs 1–3) as "Loranthaceae gen. et spec. indet." Pollen very similar to this fossil pollen can be found in two extant species of the Lorantheae: *Amyema gibberula* (type genus of Amyeminae, Clade I according Vidal-Russell & Nickrent 2008a) and *Helixanthera kirkii* (Grímsson, Grimm & Zetter 2017). Both species are similar in outline (convex-triangular, emarginate) and sculpturing (margo indistinct, with similar sculpturing than adjacent mesocolpium). In LM, *Amyema* shows a distinct hexagonal thickening of the polar nexine, whereas in *Helixanthera* the thickening covers a larger area of the grain and is most dominant in the intercolpial areas; the latter can be seen in the fossil pollen. The flanks of the equatorial apices in the equatorial plain are straight in *Helixanthera* and the fossil, whereas they are continuously curved in *Amyema*. In addition, the

polar depression in *Helixanthera* and the fossil are identical in all details in SEM (Fig. 6C, D, F), whereas in *Amyema* the polar margo is more distinct and shows three small triangular protrusions (Fig. 6E).

Use as age constraint—The phylogenetic position of *Helixanthera* within the core Lorantheae is uncertain. Nucleotide data has been produced for three species including *H. kirkii*, but the data are partly problematic and too fragmentary. *Helixanthera kirkii* (only nuclear data available, only species palynologically studied so far) nests deep within the Lorantheae core clade, and *H. parasitica* (only plastid data available) is sequentially divergent from all Lorantheae and effectively unplaced (see Fig. 7 and File S1 for further details). The third and best covered species, *H. coccinea*, groups with species of *Dendrophthoe* in agreement with the current systematic scheme, but its pollen is yet to be studied. Thus, *Helixanthera* has not been included in the taxon-reduced species-consensus dataset used here for the molecular dating. A conservative use could be constraining the minimum age of the MRCA of the Clade J (i.e. Scurrulinae, Dendrophthoinae, Emelianthinae, and Tapinanthinae; see *Discussion*).

Inferences

Basic signal in the harvested molecular data (Fig. 7)

Our inferences based on species-consensus sequences and different sets of data (see File S1 and files included in OSA) revealed no highly supported conflict between the nuclear and plastid gene regions. Inclusion or exclusion of the most divergent, length-polymorphic non-coding (plastid) trnLLF region showed little effect on the optimised ML topologies and BS support values. When not including any long-branching outgroups, the data largely fails to group the root parasitic taxa, hence, lack support for a root parasitic grade. An according subtree (e.g. Su et al. 2015, fig. 1B) draws its support exclusively from the *matK* gene data and is enforced if sistergroups of the Loranthaceae are included (Grímsson, Grimm & Zetter 2017, file S6). Overall, the single- and oligo-gene species-consensus trees showed the same principal topology as earlier found using genus-consensus sequences (Grímsson, Grimm & Zetter 2017, figs 2, 3). However, species of the same genus were not necessarily reconstructed as siblings. In case of *Helixanthera, Psittacanthus* (nuclear and plastid data), and *Plicosepalus* (plastid data only), the branches separating the putative siblings received no high support, but did so in case of *Amyema,*

Tapinanthus (nuclear and plastid data), *Amylotheca, Lepidaria,* and *Oncocalyx* (plastid data only). In terms of genetic-phylogenetic distances, the species of *Helixanthera* show the least coherence at the genus level. Aside from this, several clades were consistently reconstructed and usually received moderately high to unambiguous support (BS ≥ 70) from different data sets (Fig. 7): (*i–iv*) the Old World Lorantheae with three subclades (Loranthinae, Ileostylinae, core Lorantheae), *(v–vi)* the Amyeminae (except *Baratranthus axanthus*) and Scurrulinae within the core Lorantheae; *(vii)* the New World Psittacanthinae (except for *Aetanthus*, which is poorly sampled in our data set); and *(ix)* the Elytrantheae (poorly supported based on nuclear data due to faint discriminating signals). The positions of the other mostly monotypic genera of the family remained unresolved; alternative splits regarding deep relationships generally received low support. A detailed account regarding topological ambiguity of inferences using the currently available molecular data can be found in File S5.

The divergence in the covered gene regions is substantial (see branch-lengths in Fig. 7); the resulting terminal 'noise' appears to obscure signal that may allow discriminating deeper phylogenetic splits. This may explain to some degree, in addition to the relatively high proportion of missing data, the low resolution capacity of the species-level data sets. When the taxon set was reduced to only those species with full data coverage, support along the backbone and towards the leaves of the Loranthaceae tree increased. This reduction also showed a positive effect on the dating: using the complete taxon set and matrices with numerous data gaps, ESS values converged very slowly (rooting scenarios 1 and 3) or not at all (rooting scenario 2; see also File S1).

Alternative clock-based roots

For four of the five comprehensive datasets (all taxa, different sets of gene samples), the clock-inferred root was placed between the predominately Old World Lorantheae and a mostly southern hemispheric, American-Australasian clade collecting all three root parasitic genera and the members of the other two aerial parasitic tribes, the (probably paraphyletic) Psittacantheae and (putatively monophyletic) Elytrantheae (Table 2). In the case of the most-inclusive data set (all taxa, all gene regions), the root was shifted by two nodes and placed within the Lorantheae subtree, splitting the genetically divergent subtribes Loranthinae and Ileostylinae from the remainder of the Lorantheae (= Clade J according to Vidal-Russell & Nickrent 2008a). The

subsequent evolutionary scenario would imply that root parasites and other southern hemispheric lineages share an ancestor with only the Loranthinae and Ileostylinae, hence, a paraphyletic Lorantheae tribe, which is highly unlikely (Nickrent et al. 2010; Su et al. 2015; Grímsson, Grimm & Zetter 2017). This alternative root was not further considered. In contrast to these roots, the taxon-reduced, less "gappy" dataset (42 species covering, at least partly, all included gene regions) recovered the outgroup-inferred root, with *Nuytsia* as sister to all other loranths.

Temporal framework for pollen evolution in Loranthaceae (Figs 8–9; Table 3)

Following our clock-rooting results and those of earlier studies, we applied three different root constraints to judge potential effects of topological uncertainties regarding the primary relationships on the dating estimates. In addition, we constrained our data to the topology of the Loranthaceae subtree as showed in Su et al. (2015; scenario 4), which—according to an expert on the group—is the most correct one to date (Anonymous, pers. comm., 2016; but see Grímsson, Grimm & Zetter 2017, file S6). We find that independent of the position of the root and exact structure of the backbone topology, primary divergences in Loranthaceae were terminated by the end of the Eocene at the latest (Table 3). The primary radiation and isolation of lineages, including potential multiple transitions from root to branch (aerial) parasites, agrees well with the final phase of the Gondwana breakup. Phases of increased diversification (number of coexisting lineages) and stagnation coincide with key events in Cenozoic climate and vegetation evolution (Fig. 8). Most crown group radiation, the formation of the modern genera, apparently happened not later than the Miocene. Based on the limited species coverage, it is impossible to estimate when intra-generic radiation stepped in and at which point closer related genera isolated and diverged.

Comparison of Bayes factors showed that rooting scenario 3, the pollen-informed root, is decisively better (according Kass & Raftery 1995) than the tested alternatives (Table 4). Thus, we chose rooting scenario 3 as the basis for our discussion and conclusion. The divergence between *Tupeia* (A-type pollen) and Loranthaceae with B-type pollen is placed in the early Eocene (~50 Ma; Fig. 9, Table 3). A primary radiation involving the formation of an essentially Old World (Lorantheae) and New World clade (root parasites, Elytrantheae, Psittacantheae) followed shortly after (less than 2 myrs) and, subsequently, the first divergences in the New World clade (≥ 43 Ma; Fig. 9). Crown group radiation in the Lorantheae started in the late

Eocene (≥ 38 Ma) at the latest; the subclades and monotypic lineages (subtribes Psittacanthinae, Ligarinae, Notantherinae) of the probably paraphyletic Psittacantheae diverged about the same time. A second major radiation phase took place ~10 myrs later (latest in the Oligocene) and involved the Old World core Lorantheae (subtribes Amyeminae, Dendrophthoinae, Emelianthinae, Scurrulinae, Tapinanthinae) and New World Elytrantheae. Crown group radiation, the formation of lineages equalling most modern genera commenced at about the same time and lasted till the mid-Miocene (≥ 9 Ma). In general, the genera root deeper (are older) in the (mostly) South American Psittacanthinae than in the Old World Lorantheae sublineages and the (mainly) Australasian Elytrantheae. Generic diversification culminates in the early to mid-Miocene, a time of ameliorated global climate.

Historical Biogeography (Figs 10–11)

Pollen studied using SEM and subsequent node dating (Figs 8, 9; Table 3) indicate that several major lineages of Loranthaceae were present in the Northern Hemisphere by the middle Eocene (Fig. 10A). The Eocene pollen record includes representatives of extinct or ancestral lineages with affinities to root-parasitic genera such as *Nuytsia*/Nuytsieae but possibly also the Lorantheae (Miller Clay Pit MT1, Stolzenbach MT, Profen MT1). In addition, today's exclusively epiphytic lineages are present: Psittacanthinae in North America/Greenland (Miller Clay Pit MT2, MT3, Aamaruutissaa MT), *Notanthera* and Elytrantheae in Central Europe (Profen MT3, MT4 and MT5), and core group Lorantheae in East Asia (Changchang MT). All these records represent the earliest unequivocal fossil records of their respective groups. At least one of these lineages, the ancestral/extinct lineage bridging between root parasites and Lorantheae, persisted in Eurasia during the late Eocene and Oligocene (Theiss MT, Altmittweida MT; Fig. 10B) until today. These younger pollen types, which were not used as node age priors, are in good agreement with the dating estimates (Fig. 9). Furthermore, we noticed that none of the putatively derived pollen morphologies characteristic for certain members of the Psittacanthinae (compact B-type, C-type and D-type pollen) and Lorantheae (Loranthinae, Tapinanthinae-Emelianthinae; ± compact B-type pollen, B-type pollen with minute sculpturing, heteropolar grains) have been found (so far) in the older strata. Pollen records from the Miocene onwards, studied using LM and possibly representing a large range of Loranthaceae lineages with a B-type pollen, fall within the modern distribution area (Fig. 11), and potentially include

such B types (File S4). The most derived C- and D-type pollen characteristic for *Dendropemon, Passovia* p.p. and *Oryctanthus*, which should be straightforwardly recognised with LM only, is rare and only known from late Miocene/sub-recent sedimentary rock formations. The dated trees predict an Oligocene/early Miocene age for the MRCA of *Passovia pyrifolia* and *Oryctanthus* (Fig. 9). If Loranthaceae with A-type pollen contributed to the pollen record of the family, they would not have been recognised as Loranthaceae, hence, are not included in our maps and File S4.

Well-resolved major clades of Loranthaceae are restricted to one or two adjacent biogeographic regions (Fig. 11). Except for *Nuytsia*/Nuytsieae (today only found in southwestern Australia), the fossil pollen records essentially reflect the modern situation, only extending the range of the respective New World and Old World lineages to higher latitudes of the Northern Hemisphere.

Discussion

Diagnostic value of Loranthaceae pollen for tracing modern lineages back in time

Pollen of various modern Loranthaceae have been studied using light (LM), transmission electron- (TEM) and scanning-electron microscopy (SEM) (Feuer & Kuijt 1978; Feuer & Kuijt 1979; Feuer & Kuijt 1980; Feuer & Kuijt 1985; Kuijt 1988; Liu & Qiu 1993; Han, Zhang & Hao 2004; Roldán & Kuijt 2005; Caires 2012; Grímsson, Grimm & Zetter 2017). In general, pollen of Loranthaceae—and other Santalales—reflect phylogenetic relationships and genetic-phylogenetic distances (Grímsson, Grimm & Zetter 2017), which make them a valuable asset for biogeographic and dating studies. Some genera of putatively early diverging Loranthaceae lineages such as *Nuytsia* (monotypic Nuytsieae), *Atkinsonia* (bitypic Gaiadendreae, not resolved as clade in the molecular trees), and the Psittacantheae *Notanthera* (bitypic Nothanderinae), *Ligaria* and *Tristerix* (Ligarinae, not resolved as sibling genera), and *Tripodanthus*, *Dendropemon*, *Orycanthus* and *Passovia* p.p. (Psittacanthinae), show unique pollen types that have not been found in any other studied genus so far. Moreover, there is no indication that identical/highly similar pollen types evolved convergently in non-related Loranthaceae (or other

Santalales). Non-unique pollen types are typically found in genera which are either part of the same, well-supported molecular clade (core Lorantheae; Elythrantheae; Psittacanthinae subclades), or shared with genera where the molecular data is indecisive regarding their exact phylogenetic position (Grímsson, Grimm & Zetter 2017; this study).

Even though the modern situation makes it unlikely that—in the past—extinct lineages of Santalales or Loranthaceae have produced pollen mimicking those of modern, extant, but not closely related lineages, one needs to consider the possibility that a modern genus may have kept a (more) primitive ('plesiomorphic') pollen type of its evolutionary lineage. The Eocene and Oligocene pollen grains documented in this study show morphologies *(i)* not found in any modern taxon studied so far (Stolzenbach MT, Profen MT1, Theiss MT), or *(ii)* found exclusively in a single modern genus (monotypic *Nuytsia*: Miller Clay Pit MT1, *Tripodanthus* with three extant species: Miller Clay Pit MT2, MT3, Aamaruutissaa MT; monotypic *Notanthera*: Profen MT2; phylogenetically problematic, see Fig. 7; *Helixanthera*: Altmittweida MT), or *(iii)* are limited to a modern lineage (Elytrantheae: Profen MT3–5; core Lorantheae: Changchang MT) with none of the other so far studied modern species having an identical pollen.

Extinct or ancestral pollen morphs of the Eocene and Oligocene of Europe—The shared pollen type of the South American root parasite *Gaiadendron* and the eastern Australian Lorantheae *Muellerina* (one of two genera in the subtribe Ileostylinae, the other has not been palynologically studied thus far) is a candidate for an ancestral, primitive and shared ('symplesiomorphic') morphology. The pollen of these two genetically and morphologically distinct modern genera are indistinct (Nickrent et al. 2010; Su et al. 2015, fig. 2; Grímsson, Grimm & Zetter 2017). The distinctly striate margo is a feature only seen in a few isolated, early diverging (Eocene) modern species/genera of ambiguous phylogenetic affinity (Fig. 9, Table 3). So far no modern species showed an intermediate pollen type between the putatively plesiomorphic *Gaidendron-Muellerina* pollen and the derived pollen characterising other members of the Lorantheae, e.g. the characteristically weakly oblate pollen of *Loranthus*. The Stolzenbach MT, Profen MT1, and Theiss MT of the Eocene and Oligocene of (central) Europe are equally small and share certain ornamental characteristics with the pollen of *Gaiadendron-Muellerina* such as a distinctly striate margo. Deviating features, e.g. (more) minute sculpturing of the mesocolpium, are shared with other members of the Lorantheae. This could make them

candidates for an extinct lineage related to Lorantheae or ancestors of the Lorantheae subclades. At about the same time, more derived Lorantheae pollen grains can be found in the Eocene of East Asia (Changchang MT) and the Oligocene of Germany (Altmittweida MT), with clear affinities to the core Lorantheae, hence providing conservative minimum estimates for the Lorantheae crown age, i.e. the divergence between Loranthinae, Ileostylinae, and core Lorantheae. Our dating estimates also indicate that there was a time gap of ca. 10 myrs between the formation and initial radiation of the Lorantheae and their subsequent diversification (Fig. 9, Table 3). Our current working hypothesis is that the Stolzenbach MT, Profen MT1, and Theiss MT, do in fact represent extinct sister lineages or precursors of the modern Old World Lorantheae (e.g. the Loranthinae). Whether these Loranthaceae extended into Africa or not, is unknown. The divergence between the (East Asian) Scurrulinae and the (mostly) African Tapinanthinae and Emelianthinae is placed in the Oligocene (Fig. 9), a time when substantial global cooling triggered the retreat of subtropical and tropical forests to low latitudes (Mai 1995; Zachos et al. 2001). This event may have triggered the isolation between both clades and lead to the extinction of the ancestral pollen morphologies. Unfortunately, Africa is palaeo-palynologically understudied, so we do not know at which time the African Lorantheae with pollen grains typical for their modern members established. SEM studies of African palynofloras with Loranthaceae pollen from the Oligocene to Pliocene are needed.

Pollen of *Tripodanthus*, a putative living palyno-fossil—Another case of a modern genus that conserved a primitive pollen morphology is evident from the Eocene pollen from North America and Greenland (Miller Clay Pit MT1, MT2; Aamaruutissaa MT). These pollen are highly similar to identical to pollen of two, out of three, species of the modern South American genus *Tripodanthus*; the third species has a more compact pollen somewhat similar to that of small-flowered species of the Psittacanthinae (Fig. S4; Feuer & Kuijt 1985; Roldán & Kuijt 2005; Amico et al. 2012; Grímsson, Grimm & Zetter 2017). *Tripodanthus* is one of the earliest diverging Psittacanthinae (Figs 7, 9; Vidal-Russell & Nickrent 2008a; Grímsson, Grimm & Zetter 2017). Pollen in the other represented genera of the Psittacanthinae (*Passovia, Dendropemon, Struthanthus, Oryctanthus*) appears strongly derived in comparison to that of *Tripodanthus* and part of *Psittacanthus* (Feuer & Kuijt 1979; Feuer & Kuijt 1985), and includes types that could be unambiguously identified under LM. However, according pollen have so far not been reported from the fossil record except for youngest-most strata (Bartlett & Barghoorn

1973; Graham 1990; File S4). Moreover, the current molecular data covers only a very limited fraction of the species in the Psittacanthinae, a clade palynologically well studied and diverse. So, at the moment, we lack a sound molecular framework to test hypotheses about pollen evolution within the group, and the group is genetically undersampled. Even so, our set of ML inferences highlights the shortcoming of the current generic concepts used for the group (Fig. 7; Files S1, S5). In conclusion, the Eocene *Tripodanthus*-like pollen of North America and Greenland may have been produced by extinct or ancestral members of the Psittacanthinae, rather than an ancient member of *Tripodanthus.* It may merely confirm the existence of the New World Psittacanthinae clade in the Eocene of North America and Greenland, and should be linked with a deeper node. Using LM, Loranthaceae pollen (*Gothanipollis* sp.) has been recorded from North and South America from the early Eocene onwards (File S4 lists 17 records), which may well reveal different forms of Psittacanthinae pollen, or of less diverse New World lineages, if re-studied using SEM.

Data-inherent shortcomings

The data assembled for our study from gene banks does not allow drawing any conclusions at and below the genus level. Genus-level data are limited, and in several cases where more than a single species (or individual) has been sequenced of the same genus, the genera do not show a high coherence when it comes to tree inferences (Fig. 7). This will become a problem when studying pollen grains from younger strata, which, increasingly, may show forms identical to one or more modern genera. For instance, our assessment of the Altmittweida MT is based on its similarity to the pollen of *Amyema* and *Helixanthera* figured in Grímsson, Grimm & Zetter (2017). In that study, material was used from vouchers identified as *Amyema gibberula,* the only species of the Amyeminae clade studied so far palynologically, and *Helixanthera kirkii.* According to our species-level analyses, species of neither of the two genera are resolved as sibling species. As exemplified in Figure 7, the two or three sequenced species of *Amyema* are resolved at different placements in the Amyeminae subtree, but *A. gibberula* has not been sequenced at all. *Helixanthera kirkii* has only been sampled for nuclear data, and is placed far (phylogenetically speaking) from its congeners, which are scattered across the core Lorantheae subtree. Lacking any comparative data it cannot be judged if these placements are genuine, or if one (or several) of the species were misidentified/-associated (generic concepts are volatile in

Loranthaceae, see synonymy lists provided by Tropicos.org 2016). Thus, based on the available pollen of the Lorantheae and their established genetic affinities as members of the same clade, we can only assume with some certainty that the Altmittweida MT is a likely representative of the core Lorantheae, but not if it is a congener of *Helixanthera* or closer related to (part of) that genus. We also cannot judge to which degree *Helixanthera* pollen can be considered derived/unique enough within the core Lorantheae to warrant the association of a fossil pollen with a modern genus.

Furthermore, we can only rely on fossil pollen of several northern hemispheric localities; localities we have been studying in the last years. But most of the extant, and potentially extinct, diversity of Loranthaceae lies in the Southern Hemisphere (Figs 10–11). South America, and in particular Africa, are much less studied palynologically than e.g. Europe, and there is little to no tradition of using SEM to study fossil pollen records in the Americas or Australasia (but see Ferguson et al. 2009; Bouchal, Zetter & Denk 2016; del Carmen Zamaloa & Fernández 2016). Nevertheless, there are records of Loranthaceae pollen from these areas, and including Antarctica (File S4), covering anything between the early Eocene and Holocene. Re-studying at least some of these assemblages using high-resolution SEM photographing could provide much needed evidence for the distribution of different Loranthaceae lineages back in time. Particular, in case of South America, fossil pollen can be straightforwardly compared to the substantial variation seen in the modern genera and species at hand of the seminal works of Feuer & Kuijt (1979, 1980, 1985). Most interesting would be to pinpoint the earliest occurrences of the compact B-type pollen characteristic for *Cladocolea-Struthanthus* lineage or the strongly derived C- and D-type pollen of the *Passovia pyrifolia-Dendropemon-Orycthanthus* clade. Moreover, pollen assigned to Santalaceae or Viscaceae under LM may in fact be Loranthaceae Pollen Type A. Missing is, however, comprehensive molecular data on the Psittacanthinae at the intra-generic level and on species still included in *Phthirusa* (according Kuijt 2011; see e.g. Fig. 7). A detailed molecular-phylogenetic framework would be necessary to depicting evolutionary trends in pollen morphology of this group and identify ancestral-more primitive (plesiomorphic) vs modern-derived (apomorphic) pollen morphs of this lineage in the fossil record.

A more detailed and comprehensively studied pollen record at a global scale would also provide the necessary number of fossils to test and reconstruct explicit phylogeographic scenarios for the family. Due to the data-related limitations regarding both the molecular data

and the fossil record, our dating analysis set-up can only provide absolute minimum estimates for divergence ages in the Loranthaceae. In a recent study on Osmundaceae, we observed that uncorrelated clock-inferred dates deviated from dates inferred with the recently proposed fossilised-birth-death dating approach (FBD; Heath, Huelsenbeck & Stadler 2014), with the former tending to underestimate age (Grimm et al. 2015). In contrast to traditional node dating, FBD dating recruits the entire fossil record of a focal group and seems to outperform node dating in simulation and with real-world data (Heath, Huelsenbeck & Stadler 2014; Grimm et al. 2015; Renner et al. 2016). In the case of Loranthaceae, the coverage of lineages with fossils and of the modern taxonomic diversity is insufficient for the application of FBD, although this approach would allow a more appropriate handling of the fossils, namely as members of lineages, rather than minimum age priors for MRCA. To avoid over-interpretation of the fossils regarding the latter, all fossil age constraints and estimates were used here in a conservative manner (see *Descriptions; Inferences*). More precise estimates and a larger taxon set would be needed to reconstruct explicit migration pathways for the different Loranthaceae lineages that considers the fossil record of the family.

Timing of evolution of aerial parasitism in Loranthaceae

Keeping the data-inherent shortcomings in mind and following the common notion that the modern mode of parasitism is conserved within lineages, aerial parasitism in Loranthaceae evolved at least 20 myrs earlier (Table 3) than estimated by Vidal-Russell & Nickrent (2008b); a discrepancy easily explained. In contrast to the earlier study, we can exclusively rely on ingroup fossils as age constraints, which provide direct evidence for the occurrence of several Loranthaceae lineages in the middle Eocene. Vidal-Russell & Nickrent (2008b) used two sets of fossil constraints for their dating of an all-Santalales dataset. The first set used a single fossil (*Anacolosidites* Cookson & K.Pike) to constrain the root age of an Olacaceae s.l. subclade, the former Anacolosideae (= Aptandraceae), to 70 Ma; the second set used five additional fossils and included *Cranwellia* Sat.K.Srivast. to constrain the root age of Loranthaceae to 70 Ma. [They write "*for the crown group of Loranthaceae*" in the text, p. 527, which, however, makes no sense regarding the corresponding results shown in table 2 on p. 531.] We also did not follow Vidal-Russell & Nickrent (2008b) in using a different study, i.e. Wikström, Savolainen & Chase (2001), to constrain the (ingroup) root age. Using secondary dating constraints and age priors

based on outgroup fossils typically leads to (too) young age estimates (e.g. Grimm & Renner 2013, for Betulaceae; Garzón-Orduña et al. 2015, for Solanaceae and Ithomiini). For instance, in the two families of Canellales, Canellaceae and Winteraceae, crown group estimates using ingroup fossils as age priors are about double-as-high than those inferred based on a large magnoliid dataset including only root age constraints for the Winteraceae and the order (Marquínez et al. 2009; Thomas et al. 2014; Massoni, Couvreur & Sauquet 2015; Müller et al. 2015).

Our older estimates make sense regarding the substantial genetic divergence between extant Loranthaceae and on the backdrop of Cenozoic global climate evolution and the evolutionary history of putative and potential hosts for aerial Loranthaceae: mid- to high-canopy trees (see also Fig. 8). Although some species of the Loranthaceae family seem to be linked to a specific host, the genera themselves usually parasitise a wide range of hosts, spanning different families and even orders (File S6). The colonisation potential of aerial mistletoes is high. For instance, the New Zealand endemic *Ileostylus micranthus* (Lorantheae: Ileostylinae) parasites on 47 different families including northern hemispheric lineages introduced in historic times (Norton & de Lange 1999). Australian mistletoes commonly infest two widespread, common and native tree genera (*Acacia, Eucalyptus*), but in total 256 genera are infested and species of four genera can be found on exotic (introduced) tree genera such as *Nerium*, *Quercus*, *Platanus*, *Salix*, among others (Downey 1998). All these genera are potential hosts of northern hemispheric Loranthaceae (e.g. *Loranthus europaeus*), and can be traced back at least until the Eocene (e.g. Mai 1995). For example, primary radiation and diversification of oaks—the most divers, extratropical tree genus of the Northern Hemisphere with more than 400 modern species (Nixon 1997; Huang, Zhang & Bartholomew 1999)—was finished by the end of the Eocene (Hubert et al. 2014). The general vegetation types, in which Loranthaceae are found—various sorts of subtropical to temperate, non-frost forests but also tropical savannahs— have been available through the entire Cenozoic. Most of the Eocene is characterised by a globally ameliorated climate (Zachos et al. 2001). During this time scale, tropical and subtropical forests reached a peak in their distribution, with subtropical and temperate forests reaching far north. This could have been the trigger for the global radiation of aerial parasites in Loranthaceae evidenced by the palynological record and seen in our dating experiments. In western Greenland putatively epiphytic Loranthaceae (Aamaruutissaa MT; Psittacanthinae aff. *Tripodanthus*) co-occurred with

a high variety of subtropical to temperate Fagaceae lineages including various sublineages of *Quercus* (Grímsson et al. 2015). The palynological assemblage comprising the here described *Tripodanthus*-like Aamaruutissaa MT, indicative for Psittacanthinae, covers in total representatives of c. 30 families of woody angiosperms (Grímsson et al. 2014), including many potential hosts of epiphytic Loranthaceae in modern-day extra-tropical North America and East Asia.

In contrast, the mid-Oligocene falls into a phase of global cooling and retreat of subtropical and tropical vegetation belts to low latitudes. If aerial parasitism evolved during that time in Australia as inferred by Vidal-Russell & Nickrent (2008a, 2008b; but see Barlow 1990; Vidal-Russell & Nickrent 2007), Loranthaceae would have needed to be extremely competitive to radiate at a global scale. With its (cold-)temperate to polar climate from the Oligocene onwards, Antarctica is an unlikely corridor for the global radiation of epiphytic Loranthaceae. The situation in eastern North America and Europe, two areas heavily affected by the Pleistocene climate fluctuations, indicate that Loranthaceae cannot compete with their distant sister clade Viscaceae in the temperate zone, and there is no indication that any Loranthaceae lineage ever thrived in cold-temperate/boreal climates. Long-distance dispersal via Africa or the Pacific is unlikely in the light of the modern distribution patterns (Fig. 11). All continental African species are members of the core Lorantheae, and distant relatives of the exclusively Australasian and South American lineages. The age estimates indicate that main Australasian (probably monophyletic Elytrantheae) and New World lineages (probably paraphyletic Psittacantheae) diverged around the same time (Fig. 8; Table 3), which fits with the traditional Gondwana-Breakup scenario suggested for the family (Barlow 1990; Vidal-Russell & Nickrent 2007). The Oligocene cooling may have been the final trigger to isolate the American lineages from those in the Old World and Australasia. It also may have effected transcontinental exchange between Africa and East Asia, trigger the formation of the contemporary genera (Fig. 9, Table 3, but see *Discussion* section before), and manifest the isolation of Australasian lineages.

Conclusion

Molecular age estimates have often been criticised as being too young in comparison to the fossil record. The onset of aerial parasitism in Loranthaceae, placed in the middle Oligocene by a study including all lineages of the Santalales (Vidal-Russell & Nickrent 2008b), could have been

taken for such a case. It would have invoked three difficult to understand phenomena: *(i)* Quick long-distance dispersal and rapid radiation on a global scale of a mostly tropical-subtropical lineage during a phase of global cooling. *(ii)* Host-specialisation and simultaneous colonisation of subtropical forest elements that were already evolved by the Eocene, at least 20 myrs earlier. *(iii)* The quite rich palynological record of the zoophilous Loranthaceae, with earliest reliable records in the Eocene of Australasia (south-eastern Australia, Tasmania), East Asia (Hainan, southern China), western Eurasia (Germany), the Americas (Argentina, southeastern United States) and Greenland reflects a largely lost diversity of root parasites or extinct sister lineages of extant Loranthaceae. These extinct lineages would then have been replaced, at the earliest, in the middle Oligocene (except for three refugia) in their entire range by their newly evolved aerial parasitic siblings. Using SEM-studied fossil pollen, we can push back the origin(s) of aerial parasitism to at least the middle Eocene; a time when important hosts of modern epiphytic Loranthaceae evolved and radiated, and Earth enjoyed a phase of ameliorated climate. The new dating estimates are furthermore relatively stable regarding alternative rooting scenarios for the family.

Author contributions

FG and GWG designed the study; FG, CCH, and RZ processed, determined, and analysed the pollen; GWG compiled and processed the data; PK and GWG designed the phylogenetic and dating analyses, the latter set-up by PK. All authors took part in drafting the final version of the manuscript. Artwork by FG (pollen figures) and GWG (other).

Acknowledgements

Ignacio Escapas and Benjamin Bomfleur are thanked for supplying South American literature, Kanchi Natarajan Gandhi from the IPNI team for clarifying the standard author form for the Indian palynologist Satish Srivastava. Alastair Potts is acknowledged for proof-reading the final manuscript

References

Amico GC, Vidal-Russell R, Garcia MA, Nickrent DL. 2012. Evolutionary history of South American mistletoe *Tripodanthus* (Loranthaceae) using nuclear and plastid markers. *Systematic Botany* 37:218–225.

Baele G, Lemey P, Bedford T, Rambaut A, Suchard MA, Alekseyenko AV. 2012. xxx. *Molecular Biology and Evolution* 29:2157–2167.

Baele G, Li WLS, Drummond AJ, Suchard MA, Lemey P. 2013. xxx. *Molecular Biology and Evolution* 30:239–243.

Barlow BA. 1990. Biogeographical relationships of Australia and Malesia: Loranthaceae as a model. In: Baas P, Kalkmann K, and Geesink R, eds. *The Plant Diversity of Malesia*. Dortrecht, Boston, London: Kluwer Academic Publishers, 273–292.

Bartlett AS, Barghoorn ES. 1973. Phytogeographic history of the Isthmus of Panama during the past 12,000 years (a history of vegetation, climate, and sea-level change). In: Graham A, ed. *Vegetation and Vegetational History of Northern Latin America*. Amsterdam: Elsevier Science Publishers.

Blakey RC. 2008. Gondwana paleogeography from assembly to breakup—A 500 m.y. odyssey. In: Fielding CR, Frank TD, and Isbell JL, eds. *Resolving the Late Paleozoic Ice Age in Time and Space*. Boulder: Geological Society of America, 1–28.

Bouchal JM, Zetter R, Denk T. 2016. Pollen and spores of the uppermost Eocene Florissant Formation, Colorado: a combined light and scanning electron microscopy study. *Grana* 55:179–245.

Caires CS. 2012. Estudos taxonômicos aprofundados de O*ryctanthus (*Griseb.) Eichler, O*ryctina T*iegh, e P*usillanthus K*uijt (Loranthaceae) Ph.D. Universidade de Brasília.

del Carmen Zamaloa M, Fernández CA. 2016. Pollen morphology and fossil record of the feathery mistletoe family Misodendraceae. *Grana* 55:278–285.

Downey PO. 1998. An inventory of host species for each aerial mistletoe species (Loranthaceae and Viscaceae) in Australia. *Cunninghamia* 5:685–719.

Drummond AJ, Rambaut A. 2007. BEAST: Bayesian evolutionary analysis by sampling trees. *BMC Evolutionary Biology* 7:214.

Drummond AJ, Suchard MA, Xie D, Rambaut A. 2012. Bayesian phylogenetics with BEAUti and the BEAST 1.7. *Molecular Biology and Evolution* 29:1969–1973.

Ferguson DK, Lee DE, Bannister JM, Zetter R, Jordan GJ, Vavra N, Mildenhall DC. 2009. The taphonomy of a remarkable leaf bed assemblage from the Late Oligocene–Early Miocene Gore Lignite Measures, southern New Zealand. *International Journal of Coal Geology* 83:173–181.

Feuer SM. 1977. Pollen morphology and evolution in the Santalales sen. str., a parasitic order of flowering plants Ph.D. University of Massachusetts.

Feuer SM. 1978. Aperture evolution in the genus *Ptychopetalum* Benth. (Olacaceae). *American Journal of Botany* 65:759–763.

Feuer SM. 1981. Pollen morphology and relationships of the Misodendraceae (Santalales). *Nordic Journal of Botany* 1:731–734.

Feuer SM, Kuijt J. 1978. Fine structure of mistletoe pollen I. *Eremolepidacea*, *Lepidoceras*, and *Tupeia*. *Canadian Journal of Botany* 56:2853–2864.

Feuer SM, Kuijt J. 1979. Pollen evolution in the genus *Psittacanthus* Mart. Fine structure of mistletoe pollen II. *Botaniska Notiser* 132:295–309.

Feuer SM, Kuijt J. 1980. Fine structure of mistletoe pollen III. Large-flowered neotropical Loranthaceae and their Australian relatives. *Annals of the Missouri Botanical Garden* 72:187–212.

Feuer SM, Kuijt J. 1982. Fine structure of mistletoe pollen IV. Eurasian and Australian *Viscum* L. (Viscaceae). *American Journal of Botany* 69:1–12.

Feuer SM, Kuijt J. 1985. Fine structure of mistletoe pollen VI. Small-flowered neotropical Loranthaceae. *Annals of the Missouri Botanical Garden* 72:187–212.

Feuer SM, Kuijt J, Wiens D. 1982. Fine structure of mistletoe pollen V. Madagascan and continental African *Viscum* L. (Viscaceae). *American Journal of Botany* 69:163–187.

Garzón-Orduña IJ, Silva-Brandão KL, Willmott KR, Freitas AVL, Brower AVZ. 2015. Incompatible ages for clearwing butterflies based on alternative secondary calibrations. *Systematic Biology* 64:752–767.

Göker M, Grimm GW. 2008. General functions to transform associate data to host data, and their use in phylogenetic inference from sequences with intra-individual variability. *BMC Evolutionary Biology* 8:86.

Graham A. 1990. Late Tertiary microfossil flora from the Republic of Haiti. *American Journal of Botany* 77:911–926.

Grimm GW, Kapli P, Bomfleur B, McLoughlin S, Renner SS. 2015. Using more than the oldest fossils: Dating Osmundaceae with the fossilized birth-death process. *Systematic Biology* DOI:10.1093/sysbio/syu108.

Grimm GW, Renner SS. 2013. Harvesting GenBank for a Betulaceae supermatrix, and a new chronogram for the family. *Botanical Journal of the Linnéan Society* 172:465–477.

Grimm GW, Renner SS, Stamatakis A, Hemleben V. 2006. A nuclear ribosomal DNA phylogeny of *Acer* inferred with maximum likelihood, splits graphs, and motif analyses of 606 sequences. *Evolutionary Bioinformatics* 2:279-294.

Grímsson F, Denk T, Zetter R. 2008. Pollen, fruits, and leaves of *Tetracentron* (Trochodendraceae) from the Cainozoic of Iceland and western North America and their palaeobiogeographic implications. *Grana* 47:1–14.

Grímsson F, Grimm GW, Zetter R. 2017. Evolution of pollen morphology in Loranthaceae. *Grana* DOI:10.1080/00173134.2016.1261939.

Grímsson F, Zetter R, Grimm GW, Krarup Pedersen G, Pedersen AK, Denk T. 2015. Fagaceae pollen from the early Cenozoic of West Greenland: revisiting Engler's and Chaney's Arcto-Tertiary hypotheses. *Plant Systematics and Evolution* 301:809–832.

Grímsson F, Zetter R, Pedersen GK, Pedersen AK, Denk T. 2014. Middle Eocene palaeoflora from a resinite-rich coal bed on Hareøn (Qeqertarsuatsiag), West Greenland. 9th European Palaeobotany - Palynology Conference EPPC 2014. Padova. p 86 [abstract].

Han R-L, Zhang D-X, Hao G. 2004. Pollen morphology of the Loranthaceae from China. *Acta Phytotaxonomica Sinica* 42:436–456.

Heath TA, Huelsenbeck JP, Stadler T. 2014. The fossilized birth–death process for coherent calibration of divergence-time estimates. *Proceedings of the National Academy of Sciences* 111:E2957–E2966.

Holland B, Moulton V. 2003. Consensus networks: A method for visualising incompatibilities in collections of trees. In: Benson G, and Page R, eds. *Algorithms in Bioinformatics: Third International Workshop, WABI, Budapest, Hungary Proceedings*. Berlin, Heidelberg, Stuttgart: Springer Verlag, 165-176.

Huang C, Zhang Y, Bartholomew B. 1999. Fagaceae. In: Wu Z-Y, and Raven PH, eds. *Flora of China 4 Cycadaceae through Fagaceae*. Beijing, St. Louis: Science Press and Missouri Botanical Garden Press.

Hubert F, Grimm GW, Jousselin E, Berry V, Franc A, Kremer A. 2014. Multiple nuclear genes stabilize the phylogenetic backbone of the genus *Quercus*. *Systematics and Biodiversity* 12:405–423.

Huelsenbeck JP, Bollback JP, Levine AM. 2002. Inferring the root of a phylogenetic tree. *Systematic Biology* 51:32–43.

Huson DH, Bryant D. 2006. Application of phylogenetic networks in evolutionary studies. *Molecular Biology and Evolution* 23:254-267.

Kass RE, Raftery AE. 1995. Bayes factors. *Journal of the American Statistical Association* 90:773–795.

Kmenta M. 2011. Die Mikroflora der untermiozänen Fundstelle Altmittweida, Deutschland M.Sc. M.Sc. University of Vienna.

Kuijt J. 1988. Revision of *Tristerix* (Loranthaceae). *Systematic Botany Monographs* 19:1–61.

Kuijt J. 2011. Pulling the skeleton out of the closet: resurrection of *Phthirusa* sensu Martius and consequent revival of *Passovia* (Loranthaceae). *Plant Diversity and Evolution* 129:159–211.

Liu L-F, Qiu H-X. 1993. Pollen morphology of Loranthaceae in China [in Chinese with English abstract]. *Guihaia* 13:235–245.

Macphail MK, Jordan GJ, Hopf F, Colhoun EA. 2012. When did the mistletoe family Loranthaceae become extinct in Tasmania? Review and conjecture. *Terra Australis* 34:255–269.

Maddison WP, Maddison DR. 2011. Mesquite: a modular system for evolutionary analysis. 2.75 ed.

Maguire B, Wurdack JJ, Huang Y-C. 1974. Pollen grains of some American Olacaceae. *Grana* 14:26–38.

Mai DH. 1995. *Tertiäre Vegetationsgeschichte Europas*. Jena, Stuttgart, New York: Gustav Fischer Verlag.

Manchester SR, Grímsson F, Zetter R. 2015. Assessing the fossil record of asterids in the context of our current phylogenetic framework. *Annals of the Missouri Botanical Garden* 100:329–363.

Marquínez X, Lohmann LG, Salatino MLF, Salatino A, González F. 2009. Generic relationships and dating lineages in Winteraceae based on nuclear (ITS) and plastid (rpS16 and psbA-trnH) sequence data. *Molecular Phylogenetics and Evolution* 53:435–449.

Massoni J, Couvreur TLP, Sauquet H. 2015. Five major shifts of diversification through the long evolutionary history of Magnoliidae (angiosperms). *BMC Evolutionary Biology* 15:49.

Muller J. 1981. Fossil pollen records of extant angiosperms. *Botanical Review* 47:1–142.

Müller S, Salomo K, Salazar J, Naumann J, Jaramillo MA, Neinhuis C, Feild TS, Wanke S. 2015. Intercontinental long-distance dispersal of Canellaceae from the New to the Old World revealed by a nuclear single copy gene and chloroplast loci. *Molecular Phylogenetics and Evolution* 84:205–219.

Nickrent DL. 1997 onwards. The Parasitic Plant Connection. Nickrent, D. L.

Nickrent DL, Malécot V, Vidal-Russell R, Der JP. 2010. A revised classification of Santalales. *Taxon* 9:538–558.

Nixon KC. 1997. Fagaceae. In: Flora of North America Editorial Committee, ed. *Flora of North America North of Mexico*. New York: Oxford University Press, 436-537.

Norton DA, de Lange PJ. 1999. Host specifity in parasitic mistletoes (Loranthaceae) in New Zealand. *Functional Ecology* 13:552–559.

Pattengale ND, Masoud A, Bininda-Emonds ORP, Moret BME, Stamatakis A. 2009. How many bootstrap replicates are necessary? In: Batzoglou S, ed. *RECOMB 2009*. Berlin, Heidelberg: Springer-Verlag, 184–200.

Renner SS, Grimm GW, Kapli P, Denk T. 2016. Species relationships and divergence times in beeches: New insights from the inclusion of 53 young and old fossils in a birth-death clock model. *Philosophical Transactions of the Royal Society B* DOI:10.1098/rstb.2015.0135.

Renner SS, Grimm GW, Schneeweiss GM, Stuessy TF, Ricklefs RE. 2008. Rooting and dating maples (*Acer*) with an uncorrelated-rates molecular clock: Implications for North American/Asian disjunctions. *Systematic Biology* 57:795-808.

Roldán FJ, Kuijt J. 2005. A new, red-flowered species of *Tripodanthus* (Loranthaceae) from Columbia. *Novon* 15:207–209.

Song Z-C, Wang W-M, Huang F. 2004. Fossil pollen records of extant angiosperms in China. *Botanical Review* 70:425–458.

Stamatakis A. 2014. RAxML version 8: a tool for phylogenetic analysis and post-analysis of large phylogenies. *Bioinformatics* 30:1312–1313.

Su H-J, Hu J-M, Anderson FE, Der JP, Nickrent DL. 2015. Phylogenetic relationships of Santalales with insights into the origins of holoparasitic Balanophoraceae. *Taxon* 64:491–506.

Thomas N, Bruhl JJ, Ford A, Weston PH. 2014. Molecular dating of Winteraceae reveals a complex biogeographical history involving both ancient Gondwanan vicariance and long-distance dispersal. *Journal of Biogeography* 41:894–904.

Tropicos.org. 2016. Tropicos® database. Missouri Botanical Garden.

Vidal-Russell R, Nickrent DL. 2007. The biogeographic history of Loranthaceae. *Darwiniana* 45:52–54.

Vidal-Russell R, Nickrent DL. 2008a. Evolutionary relationships in the showy mistletoe family (Loranthaceae). *American Journal of Botany* 95:1015–1029.

Vidal-Russell R, Nickrent DL. 2008b. The first mistletoes: Origins of aerial parasitism in Santalales. *Molecular Phylogenetics and Evolution* 47:523–537.

Wikström N, Savolainen V, Chase MW. 2001. Evolution of the angiosperms: Calibrating the family tree. *Proceedings of the Royal Society London: B, Biological Sciences* 268:2211–2220.

Wilson CA, Calvin CL. 2006. An origin of aerial branch parasitism in the mistletoe family, Loranthaceae. *American Journal of Botany* 93:787–796.

Zachos JC, Pagani M, Sloan L, Thomas E, Billups K. 2001. Trends, rhythms, and aberrations in global climate 65 Ma to present. *Science* 292:686-693.

Zetter R. 1989. Methodik und Bedeutung einer routinemäßig kombinierten lichtmikroskopischen und rasterelektonenmikroskopischen Untersuchung fossiler Mikrofloren. *Courier Forschungsinstitut Senckenberg* 109:41–50.

Figure 1

LM micrographs (polar views) of all fossil Loranthaceae morphotypes

(A) Miller Clay Pit MT1. (B) Miller Clay Pit MT1. (C) Miller Clay Pit MT2. (D) Miller Clay Pit MT3. (E) Aamarutissaa MT. (F) Stolzenbach MT. (G) Profen MT1. (H) Profen MT1. (I) Profen MT2. (J) Profen MT2. (K) Profen MT3. (L) Profen MT4. (M) Profen MT4. (N) Profen MT4. (O) Profen MT4. (P) Profen MT5. (Q) Profen MT5. (R) Changchang MT. (S) Changchang MT. (T) Theiss MT. (U) Theiss MT. (V) Theiss MT. (W) Theiss MT. (X) Theiss MT. (Y) Altmittweida MT. (Z) Altmittweida MT. (Ä) Altmittweida MT.

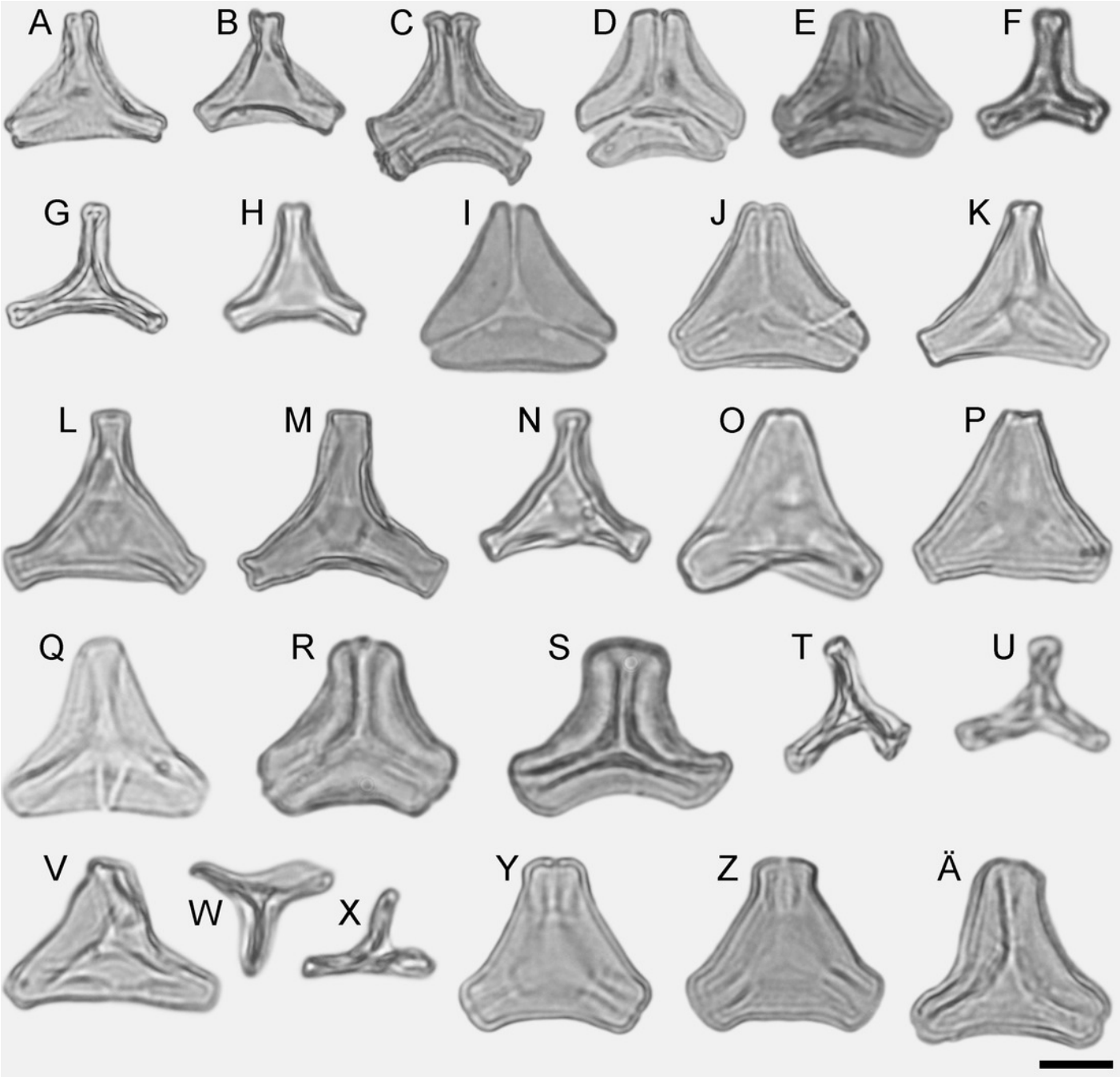
A
B
C
D
E
F
G
H
I
J
K
L
M
N
O
P
Q
R
S
T
U
V
W
X
Y
Z
Ä

Figure 2

SEM micrographs of fossil Loranthaceae pollen similar to/intermediate between root parasites and Lorantheae and comparable extant pollen

(A–D) Polar views of fossil pollen. (E–G) Polar views of extant pollen. (H–J) Close-ups of sculpturing in area of mesocolpium and along margo in fossil pollen. (K–M) Close-ups of sculpturing in area of mesocolpium and along margo in extant pollen. (A, H) Miller Clay Pit MT1. (B, I) Stolzenbach MT. (C, J) Profen MT1. (D) Theiss MT. (E, K) *Nuytsia floribunda*. (F, L) *Gaiadendron punctatum*. (G, M) *Muellerina eucalyptoides*. Scale bars: (A–M) = 1 µm.

**Note: Auto Gamma Correction was used for the image. This only affects the reviewing manuscript. See original source image if needed for review.*

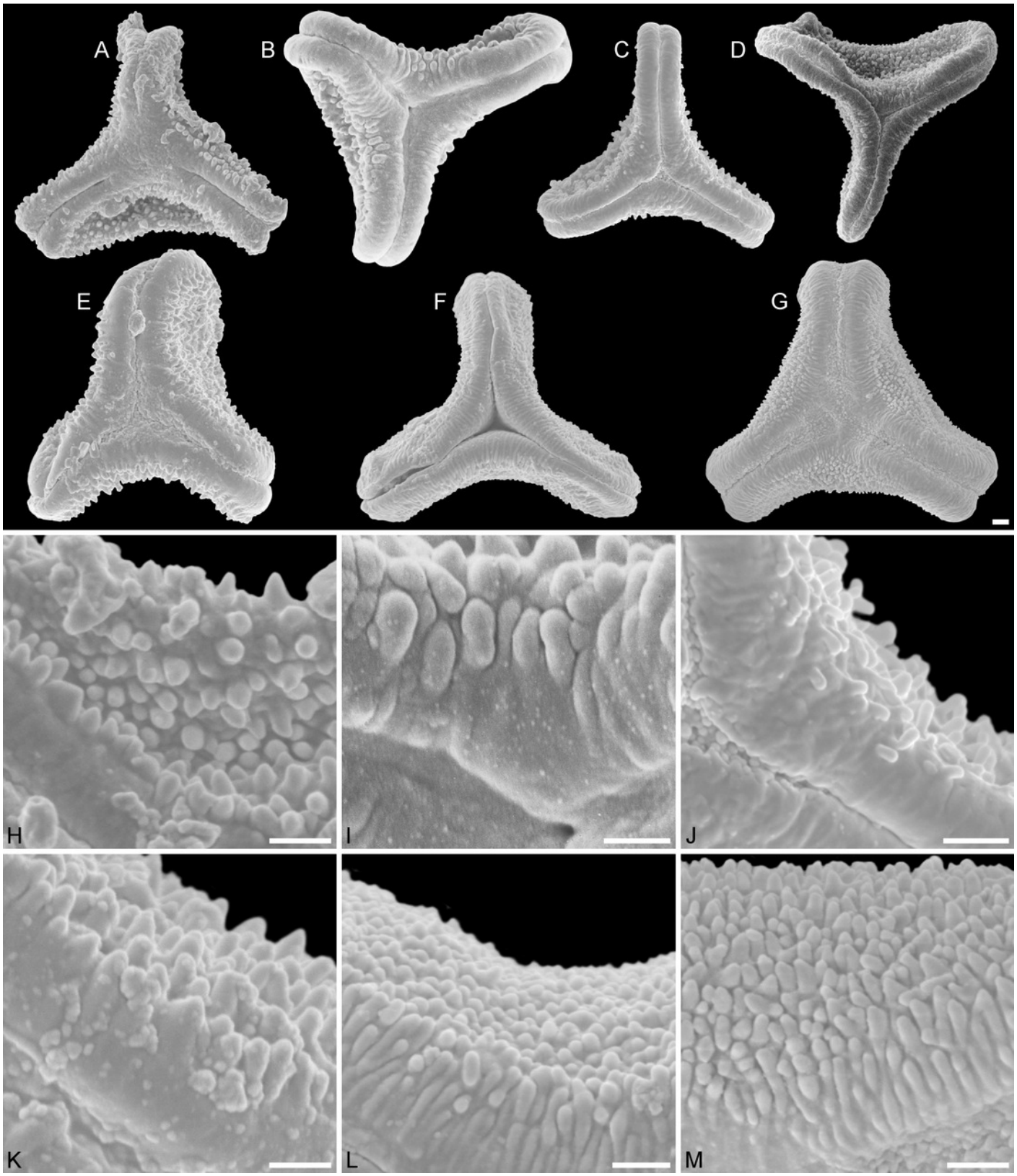
A
B
C
D
E
F
G
H
I
J
K
L
M

Figure 3

SEM micrographs of fossil Loranthaceae pollen with affinity to *Tripodanthus* and extant pollen of the genus

(A–D) Polar views of fossil pollen. (E, F) Polar views of extant pollen. (G–J) Close-ups of sculpturing in area of mesocolpium and along margo in fossil pollen. (K, L) Close-ups of sculpturing in area of mesocolpium and along margo in extant pollen. (A, G) Miller Clay Pit MT2. (B, C, H, I) Miller Clay Pit MT3. (D, J) Aamaruutissaa MT. (E, F, K, L) *Tripodanthus acutifolius*. Scale bars: (A–F) = 10 µm, (G-L) = 1 µm.

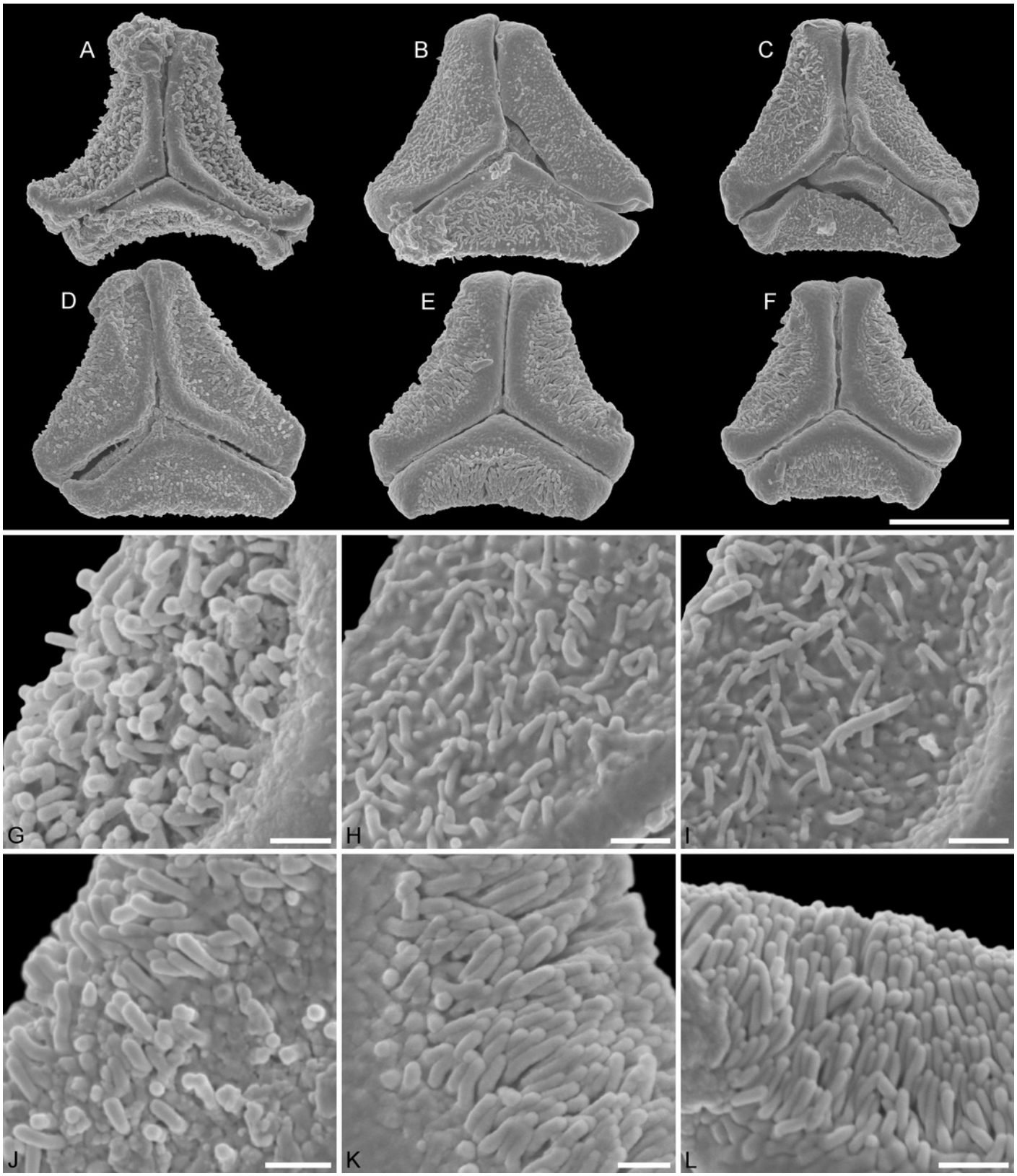
A
B
C
D
E
F
G
H
I
J
K
L

Figure 4

SEM micrographs of fossil Loranthaceae pollen with affinity to Elytrantheae and extant representatives

(A–F) Polar views of fossil pollen. (G-I) Polar views of extant pollen. (A) Profen MT2. (B) Profen MT2. (C) Profen MT3. (D) Profen MT4. (E) Profen MT4. (F). Profen MT5. (G) *Peraxilla tetrapetala*. (H) *Amylotheca* sp. (I) *Ligaria cuneifolia*. Scale bar: (A–I) = 10 µm.

**Note: Auto Gamma Correction was used for the image. This only affects the reviewing manuscript. See original source image if needed for review.*

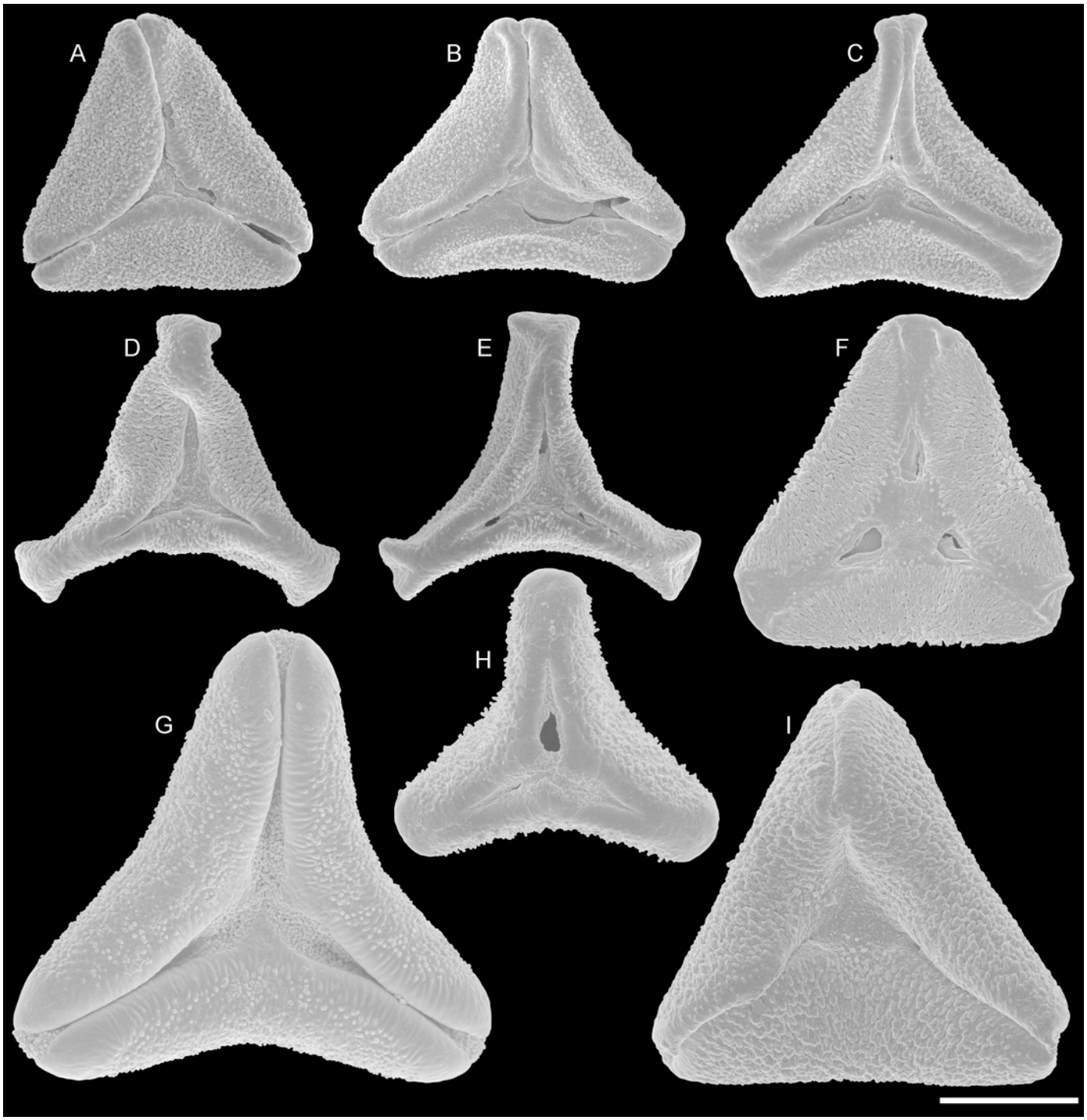
A
B
C
D
E
F
G
H
I

Figure 5

SEM micrographs of fossil Loranthaceae pollen with affinity to Elytrantheae and extant representatives

(A–E) Close-ups of sculpturing in area of mesocolpium and along margo in fossil pollen. (F–H) Close-ups of sculpturing in area of mesocolpium and along margo in extant pollen. (A) Profen MT2. (B) Profen MT2. (C) Profen MT3. (D) Profen MT4. (E) Profen MT5. (F) *Peraxilla tetrapetala*. (G) *Amylotheca* sp. (H) *Ligaria cuneifolia*. Scale bar: (A-H) = 1 µm.

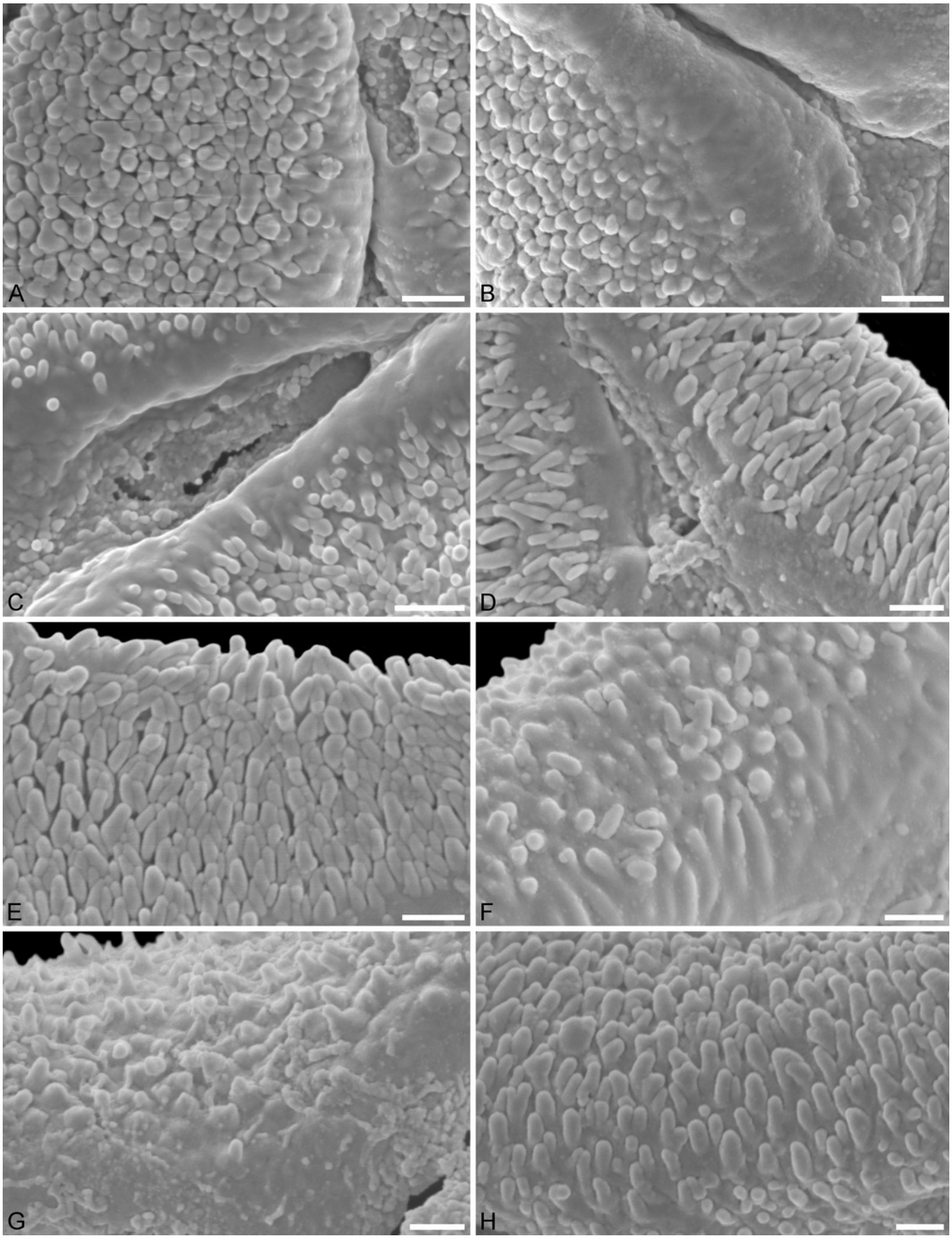
A
B
C
D
E
F
G
H

Figure 6

SEM micrographs of fossil Loranthaceae pollen with affinity to crown group Lorantheae and comparable extant pollen

(A–D) Polar views of fossil pollen. (E–G) Polar views of extant pollen. (H–J) Close-ups of sculpturing in area of mesocolpium and along margo in fossil pollen. (K–M) Close-ups of sculpturing in area of mesocolpium and along margo in extant pollen. (A, B, H, I) Changchang MT. (C, D, J) Altmittweida MT. (E, K) *Amyema gibberula*. (F, L) *Helixanthera kirkii*. (G, M) *Taxillus caloreas*. Scale bars: (A-G) = 10 µm, (H–M) = 1 µm

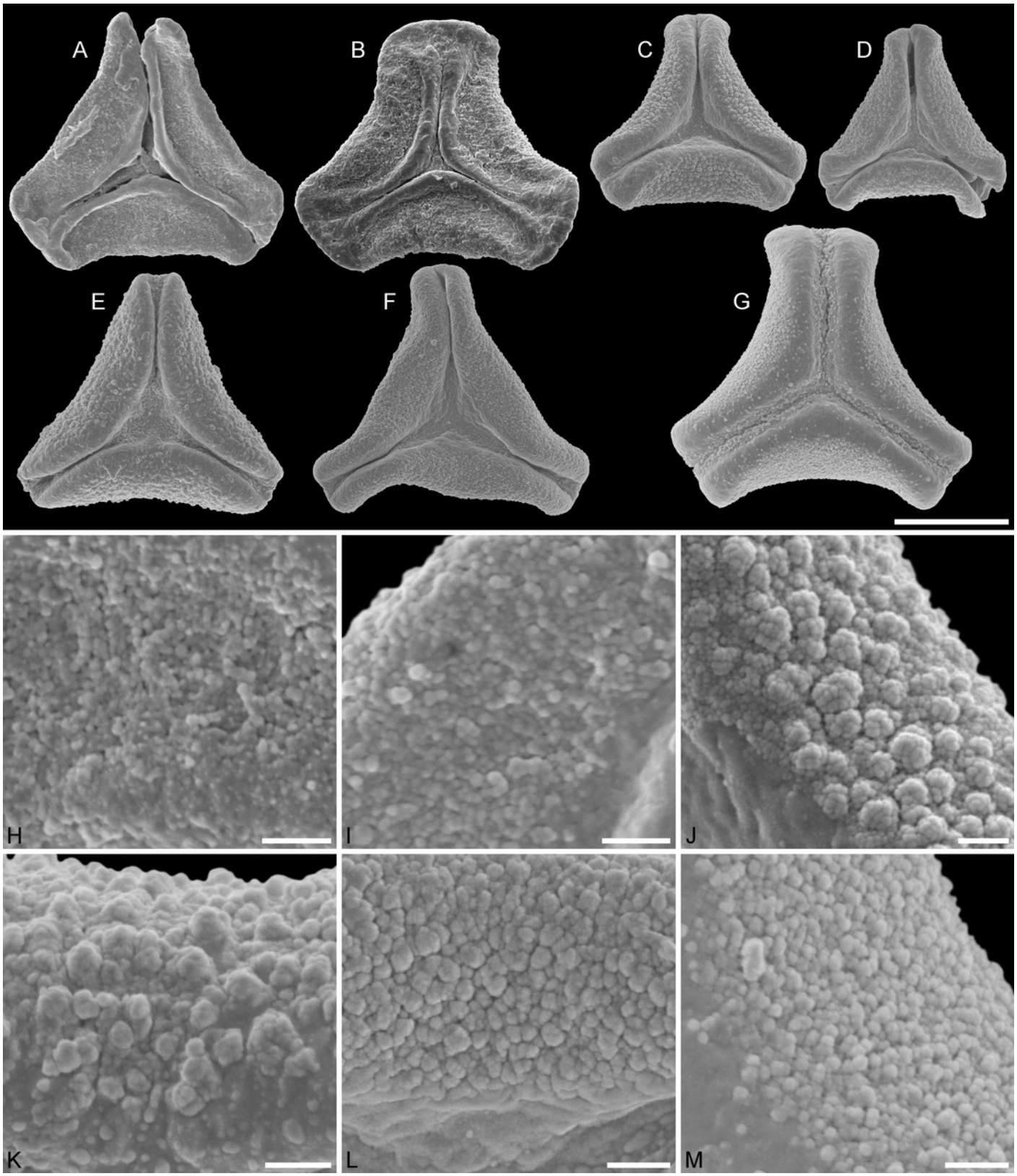
A
B
C
D
E
F
G
H
I
J
K
L
M

Figure 7

Plastid and nuclear species trees for the complete taxon set

No high-supported conflict is found; both datasets recognise the same main clades, while failing to resolve most of the deeper inter-clade relationships. Particularly, the phylogenetic position of tribes/subtribes with few, often monotypic, genera (root parasitic Nuytsieae, Gaiadendreae, aerial parasitic Ligarinae, Notantherinae, and Tupeinae) is essentially unresolved. Local differences in the topologies and odd placements are often related to species with large amount of missing data. Stippled terminal lines have been reduced by factor 2.

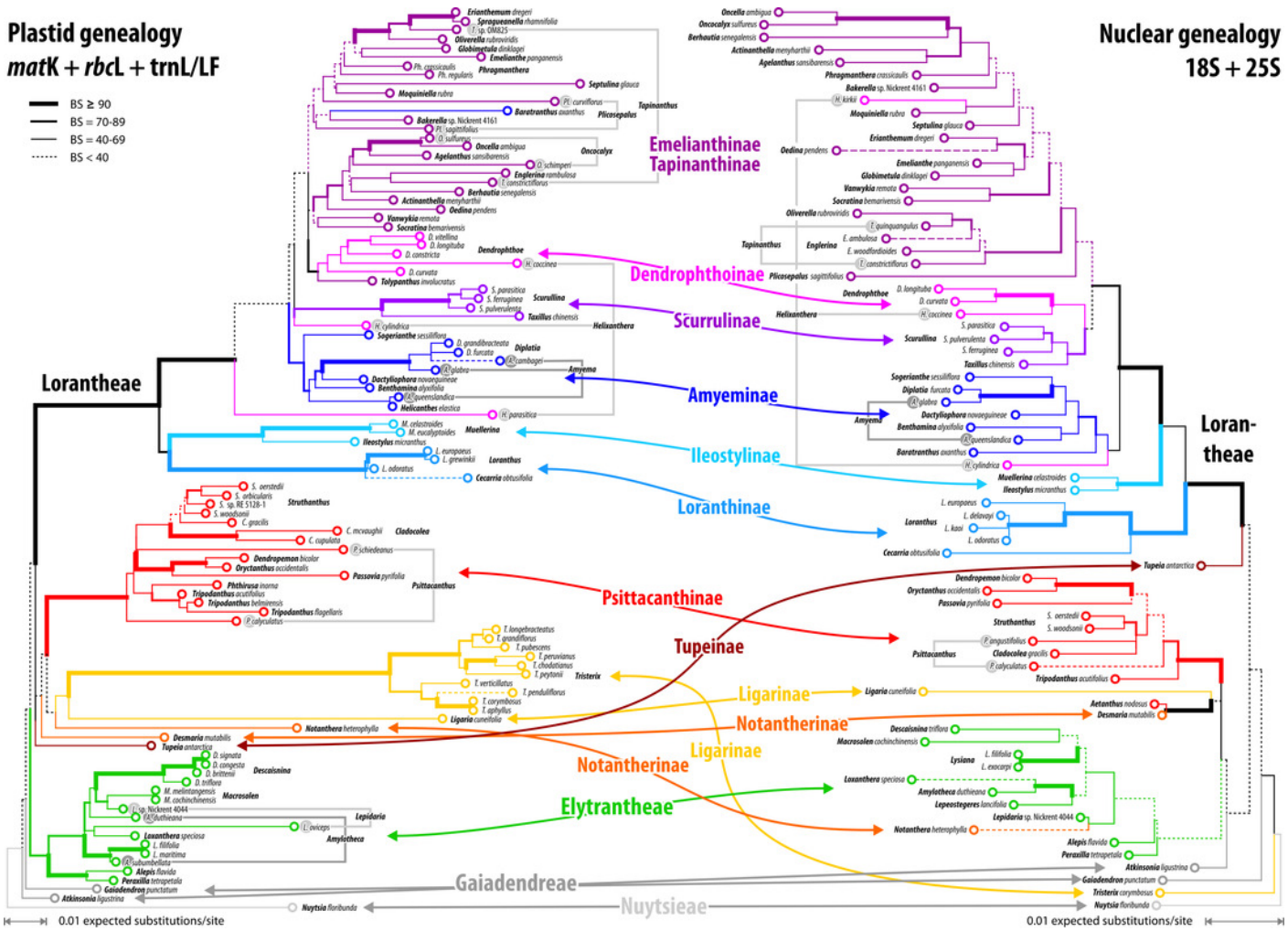

Figure 8(on next page)

Lineage-through-time plots for Loranthaceae as inferred based on three different rooting scenarios or enforcing the topology of Su et al. (2015; scenario 4)

Background shows the stable-isotope-based (marine sediments) global temperature curve with main climatic events annotated at the bottom (after Zachos et al. 2001). Increased diversification of Loranthaceae is inferred for time-scales when the global mean temperature was at least ~5° C higher than today (middle to late Eocene; late Oligocene to mid-Miocene).

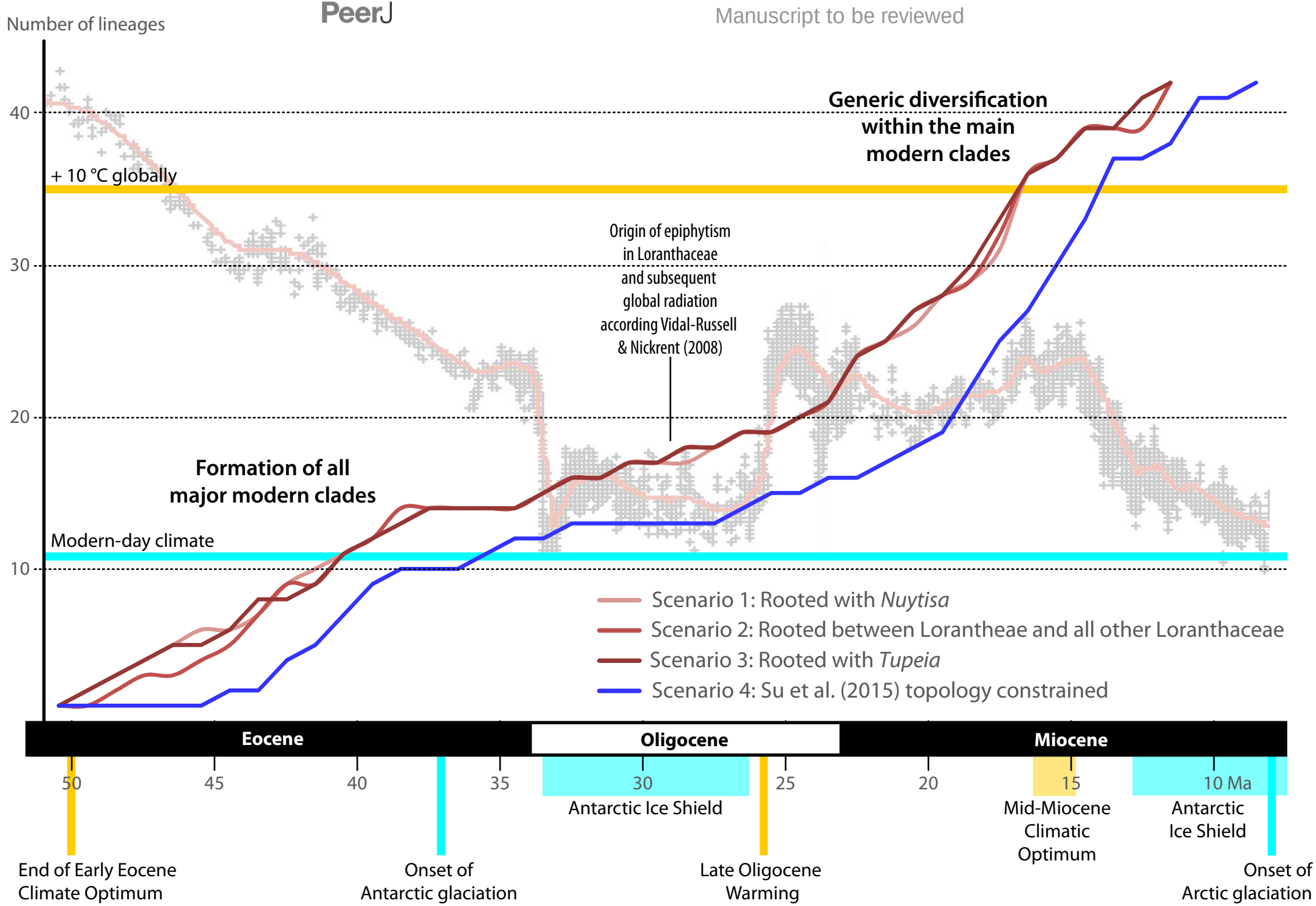
Number of lineages
40
30
20
10
+ 10 °C globally
Modern-day climate
Generic diversification within the main modern clades
Origin of epiphytism in Loranthaceae and subsequent global radiation according Vidal-Russell & Nickrent (2008)
Formation of all major modern clades
Scenario 1: Rooted with Nuytisa
Scenario 2: Rooted between Lorantheae and all other Loranthaceae
Scenario 3: Rooted with Tupeia
Scenario 4: Su et al. (2015) topology constrained
Eocene
Oligocene
Miocene
50
45
40
35
30
25
20
15
10 Ma
Antarctic Ice Shield
Mid-Miocene Climatic Optimum
Antarctic Ice Shield
End of Early Eocene Climate Optimum
Onset of Antarctic glaciation
Late Oligocene Warming
Onset of Arctic glaciation

Figure 9(on next page)

A dated phylogeny of Loranthaceae using the pollen-informed root (rooting scenario 3)

The chronogram is based on a concatenated data set including two nuclear ribosomal RNA genes (18S and 25S rDNA), two coding plastid genes (*rbc*L, *mat*K) and the trnLLF region. The taxon set has been reduced to species with sufficient data, i.e. data covering all included gene regions. Node heights (divergence ages) are medians, grey bars indicate the 95%-highest-posterior-density intervals; labels at branches indicate posterior probabilities for those branches that did not receive unambiguous support. Triangular doodles represent pollen used as age priors for the according nodes: green – Central Europe; red – North America (including Greenland); yellow – East Asia. Abbreviations: ECO = Eocene warm phase; MCO = Miocene warm phase (see Fig. 8)

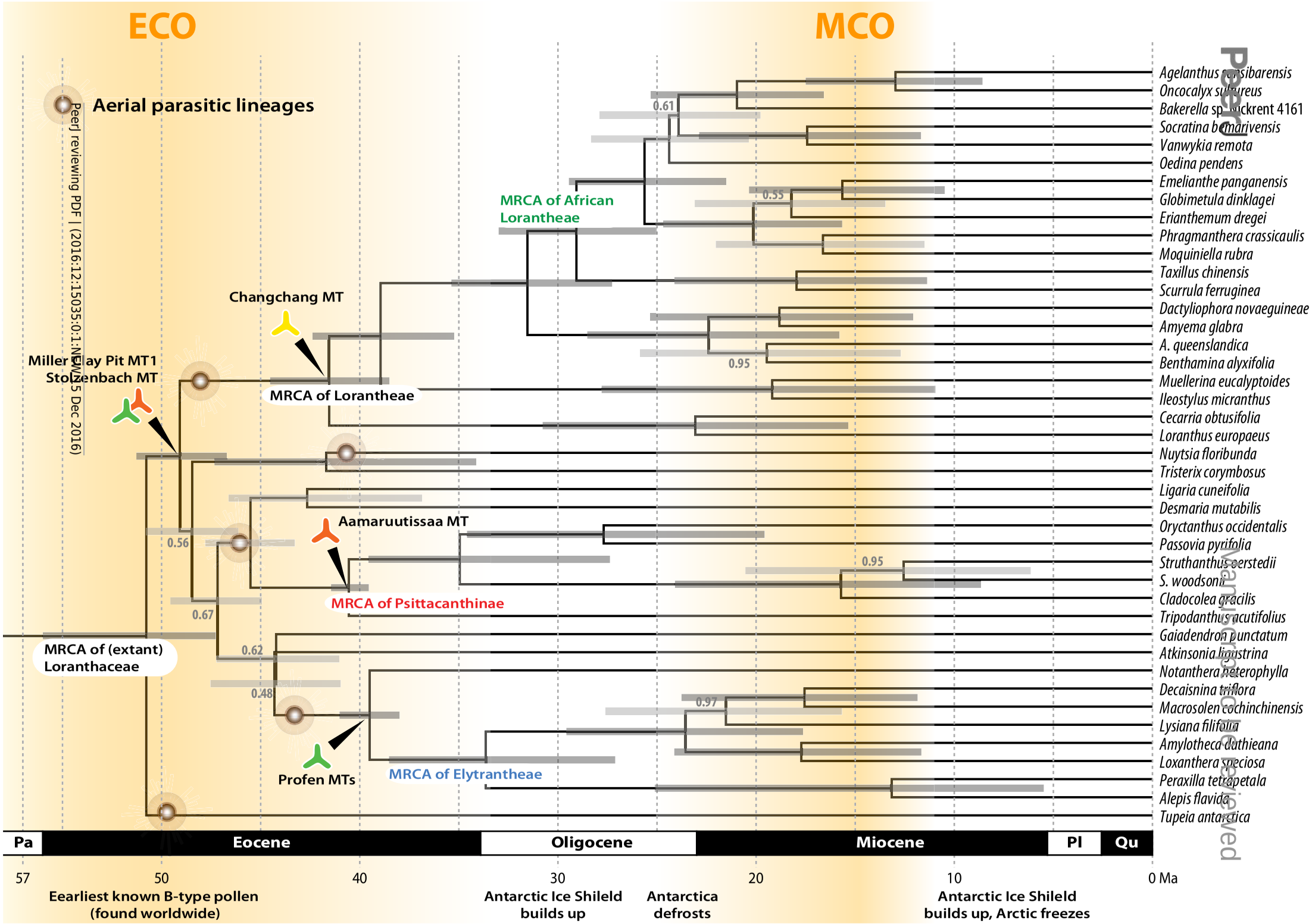

Figure 10(on next page)

Global distribution of Loranthaceae in the Paleogene, evidenced based on unequivocal palynological records

(A) Eocene. (B) Oligocene. Maps are Mollweide views, projected through the prime meridian (Blakey 2008)

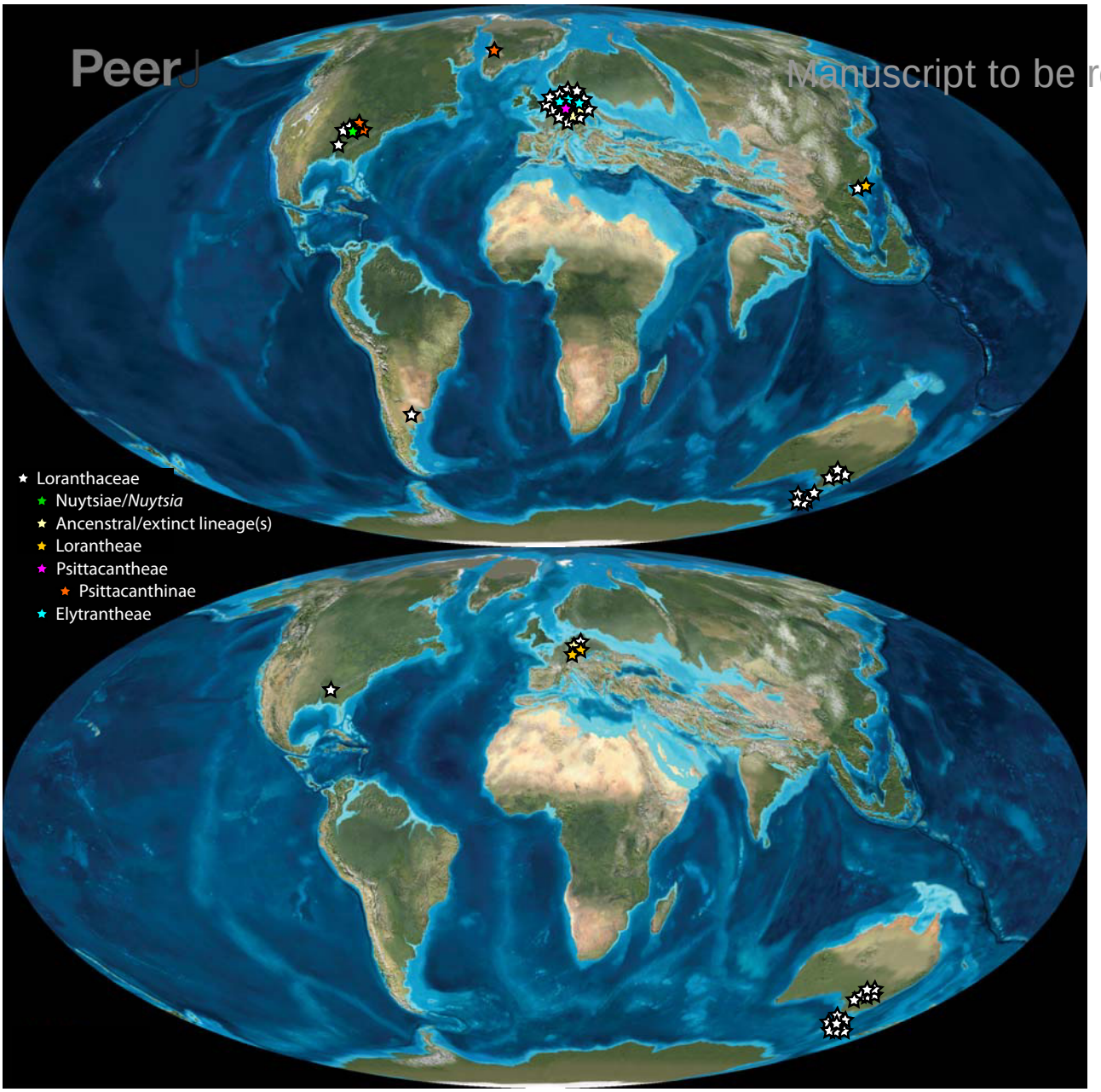

Figure 11(on next page)

Global distribution of Loranthaceae in the Neogene, evidenced based on unequivocal palynological records

(A) Miocene. (B) Pliocene to recent. Maps are Mollweide views, projected through the prime meridian (Blakey 2008)

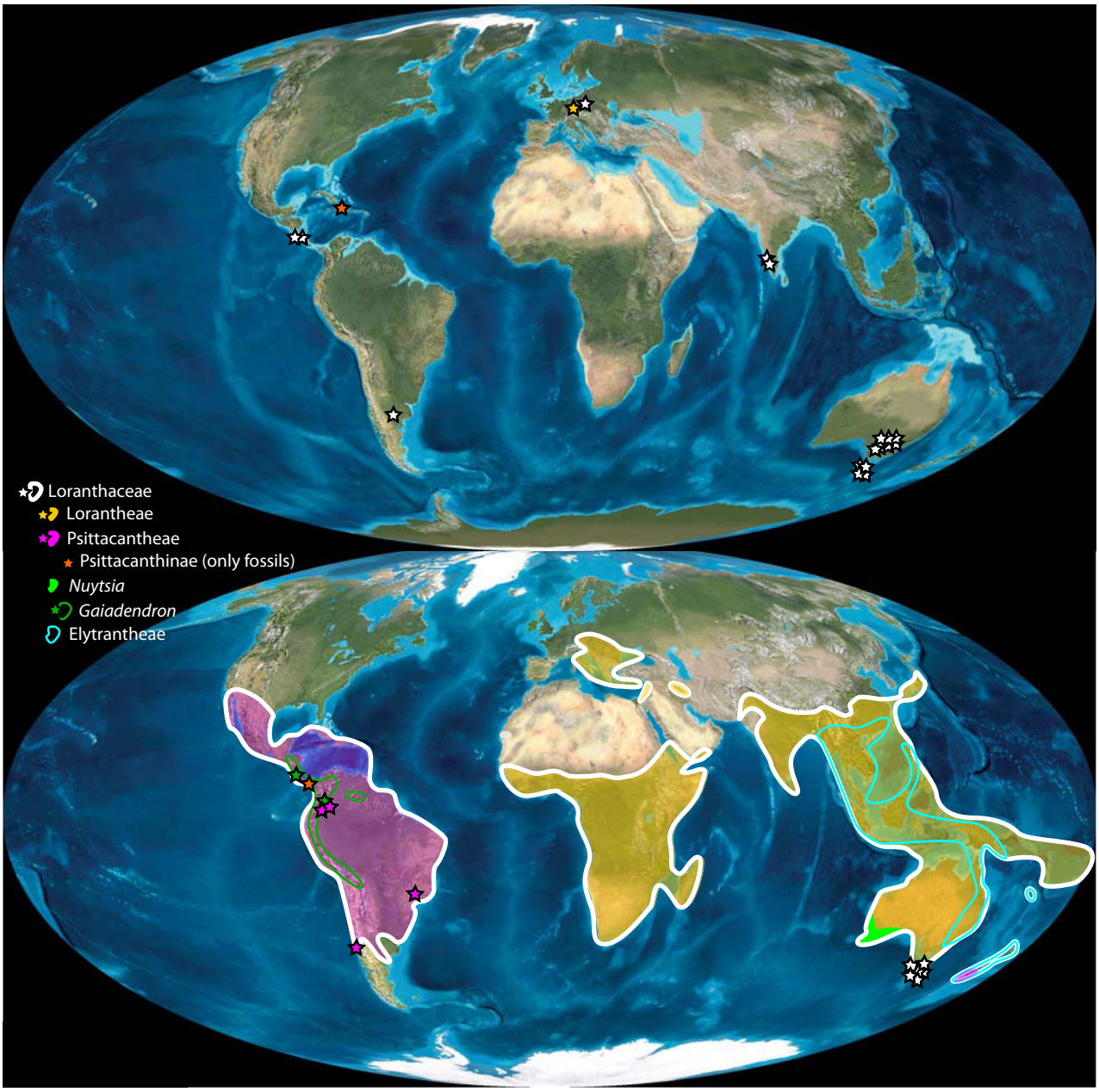
Loranthaceae
Lorantheae
Psittacantheae
Psittacanthinae (only fossils)
Nuytsia
Gaiadendron
Elytrantheae

Table 1 (on next page)

Information on sample sites

Table 1. Information on sample sites.

	Miller Clay Pit MT1-MT3	**Aamaruutissaa MT**	**Stolzenbach MT**	**Profen MT1-MT5**	**Changchang MT**	**Theiss MT**	**Altmittweida MT**
Location	Miller Clay Pit, Henry County, Tennessee, United States	Aamaruutissaa, southeast Hareøen Island, western Greenland	Stolzenbach underground coalmine, Kassel, Germany	Profen opencast mine, close to Leipzig, Germany	Changchang Basin, close to Jiazi Town, Qiongshan County, northern Hainan Island, South China	Theiss, borehole southeast of Krems, Lower Austria	Altmittweida, Saxony, Germany
Latitude and longitude (ca.)	36°13´N, 88°27´W	70°24´N, 54°41´W	51°0´N, 9°17´E	51°09´N, 12°11´E	19°38´N, 110°27´E	48°23´N, 15°41´E	50°58´N, 12°55´E
Lithostratigraphy	Claiborne Group	Hareøen Formation	Borkener coal measures	Profen Formation	Changchang Formation	Melker Series	Cottbus/Spremberg Formations
Epoch	Middle Eocene (Lutetian)	Middle Eocene (late Lutetian-early Bartonian)	Middle Eocene (Lutetian)	Middle Eocene (Bartonian)	Middle Eocene (Lutetian-Bartonian)	Middle Oligocene (Rupelian)	Late Oligocene (Chattian) / Early Miocene
Age (Ma)	47.8-41.2	42-40	47.8-41.2	41.2-38	47.8-37.8	33.9-28.1	28.1-20.44
Notes on palynofloras	Dominated by angiosperms, rich in Fagaceae, Juglandaceae, Sapotaceae, Anarcardiaceae, Olacaceae, Cannabaceae, and Altingiaceae	Diverse spore and pollen flora, rich in Cupressaceae and Angiosperms. *Fagus* , *Quercus* spp. and Castaneoideae type pollen abundant	Dominated by angiosperms, rich in Ericaceae, Fagaceae, Hamamelidaceae, Altingiaceae, Combretaceae, Burseraceae, Icacinaceae, Juglandaceae, Lecythidiaceae, and Sapotaceae	Dominated by angiosperms, rich in Anacardiaceae, Araceae, Arecaceae, Fagaceae, Sapotaceae, Symplocaceae, and Compretaceae	Diverse in angiosperms, rich in Fagaceae pollen, especially Quercoideae and Castaneoideae	Dominated by angiosperms, rich in varoius Fagaceae, Sapotaceae, Juglandaceae, Vitaceae, Malvaceae, Symplocaceae, Cornaceae, Oleaceae, and Arecaceae	Diverse in angiosperms, rich in Juglandaceae and Fagaceae genera
For further info on the geological background, stratigraphy, paleoenvironment, paleoclimate, and plant fossils (e.g.)	Potter 1976; Taylor 1989; Dilcher & Lott 2005; Wang et al. 2013	Heer 1883; Hald 1976, 1977; Schmidt et al. 2005; Dam et al. 2009; Grímsson et al. 2014a, 2014b, 2015; Manchester et al. 2015	Oschkinis and Gregor 1992; Tobien 1961; Gregor 2005; Hottenrott et al. 2010; Gregor and Oschkinis 2013; Gregor et al 2013; Manchester et al. 2015	Krutzsch and Lenk 1973; Pälchen and Walter 2011; Manchester et al. 2015	Guo 1979; Lei et al. 1992; Jin et al. 2002; Yao et al. 2009; Spicer et al. 2014	Hochuli 1978; Weber and Weiss 1983; Eschig 1992; Grímsson et al. 2012a	Engelhardt 1870; Mai and Walter 1991; Standke 2008; Kmenta 2011; Kmenta and Zetter 2013

Table 2 (on next page)

Results of the clock-rooting analyses

Table 2. Results of the clock-rooting analyses.

Species set	Gene set	Inferred root
All	All	Between Lorantheae core clade and all other Loranthaceae (including Loranthinae and Ileostylinae; not used as rooting scenario for subsequent analyses)
All	All, excluding trnLLF	Between Lorantheae and all other Loranthaceae (= rooting scenario 2)
All	Nuclear ribosomal DNAs only	Between Lorantheae and all other Loranthaceae (= rooting scenario 2)
All	Chloroplast regions only	Between Lorantheae and all other Loranthaceae (= rooting scenario 2)
All	Chloroplast genes only	Between Lorantheae and all other Loranthaceae (= rooting scenario 2)
Reduced	All	Between *Nuytsia* and all other Loranthaceae (equals outgroup inferred root; = rooting scenario 1)

Table 3 (on next page)

Results of the dating analyses using the reduced taxon data set and different rooting scenarios

Table 3. Results of the dating analyses using the reduced taxon data set and different rooting scenarios

Node	Rooting scenario 1			Rooting scenario 2			Rooting scenario 3			Scenario 4 (true tree)			Av.Medians	Abs.min	Corresponds to	
	L.b.	Mediar	U.b.	L.b.	Mediar	U.b.	L.b.	Mediar	U.b.	L.b.	Mediar	U.b.				
Loranthaceae crown	52.6	50.1	47.8	51.5	**49.1**	46.9	56.1	50.8	47.3	48.0	45.4	43.0	**48.9**	43.0	Earliest	Lutetian
Nuytsia root	52.6	50.1	47.8	50.4	48.1	45.9	47.4	41.6	34.2	48.0	**45.4**	43.0	**46.3**	34.2	Latest	Priabonian
Atkinsonia root	46.8	**43.8**	40.7	45.7	43.1	40.5	47.5	44.3	40.9	45.9	43.9	42.0	**43.8**	40.5	Early	Bartonian
Gaiadendron root	46.5	**43.7**	40.7	45.7	43.1	40.6	47.4	44.3	41.1	45.1	43.2	41.5	**43.6**	40.6	Early	Bartonian
Tristerix root	52.2	49.7	47.3	48.0	**44.4**	38.9	47.4	41.6	34.2	40.4	37.0	31.9	**43.2**	31.9	Latest	Priabonian
Tupeia root	49.7	47.2	44.8	48.0	**44.4**	38.9	56.1	50.8	47.3	42.2	39.1	32.7	**45.4**	32.7	Late	Bartonian
MRCA (aerial parasitic) New World taxa	52.2	49.7	47.3	48.7	**46.8**	44.9	50.8	48.5	46.2	42.8	41.4	40.2	**46.6**	40.2	Mid	Lutetian
MRCA *Desmaria-Ligaria*	46.0	**42.2**	36.3	45.2	41.5	36.0	46.7	42.6	36.9	42.8	41.4	40.2	**41.9**	36.0	Mid	Priabonian
Notanthera + Elytrantheae root*	46.8	**43.8**	40.7	45.7	43.1	40.5	47.5	44.3	40.9	[N/A]	[N/A]	[N/A]	**43.7**	40.5	Early	Bartonian
MRCA *Notanthera* + Elytrantheae*	41.0	**39.5**	38.0	40.9	39.4	37.8	41.0	**39.5**	38.0	44.1	42.5	41.1	**40.2**	37.8	Latest	Bartonian
Notanthera + Psittacanthinae root*	[N/A]	[N/A]	[N/A]	[N/A]	[N/A]	[N/A]	[N/A]	[N/A]	[N/A]	42.2	**40.9**	39.7	**40.9**	39.7	Early	Bartonian
MRCA *Notanthera* + Psittacanthinae*	48.6	46.4	44.3	47.4	**45.5**	43.8	49.6	47.2	44.9	41.5	40.5	39.5	**44.9**	39.5	Early	Bartonian
Psittacanthinae root	47.1	45.0	43.0	46.2	**44.4**	42.6	47.9	45.5	43.4	41.5	40.5	39.5	**43.8**	39.5	Latest	Lutetian
Psittacanthinae crown	41.4	40.4	39.5	41.3	**40.3**	39.4	41.5	40.6	39.6	29.8	22.8	16.7	**36.0**	16.7	Mid	Bartonian
Elytrantheae root	41.0	**39.5**	38.0	40.9	39.4	37.8	41.0	**39.5**	38.0	42.6	41.2	39.6	**39.9**	37.8	Latest	Bartonian
Elytrantheae crown	38.5	33.4	26.7	38.2	**33.1**	26.6	38.5	33.5	27.0	35.1	27.2	20.2	**31.8**	20.2	Early	Chattian
Lorantheae root	49.7	**47.2**	44.8	51.5	49.1	46.9	51.4	49.1	46.8	42.6	41.2	39.6	**46.7**	39.6	Mid	Lutetian
Lorantheae crown	44.2	**41.1**	37.8	45.1	41.8	38.5	44.7	41.6	38.6	38.1	35.9	33.5	**40.1**	33.5	Earliest	Priabonian
Core Lorantheae crown	35.2	**31.2**	27.0	35.9	31.6	27.4	35.6	31.7	27.4	29.8	26.5	22.9	**30.2**	22.9	Early	Chattian

Cells with same background colour refer to the same node. Abbreviations: u.b. = upper boundary, l.b. = lower boundary, of the 95%-highest-posterior-density interval
* If topology is unconstrained, *Notanthera* is placed as sister to Elytrantheae; in Scenario 4, *Notanthera* has been constrained to its correct (Anonymous, pers. comm., 2016) position as sister to Psittacanthinae (topological constraints derived from the tree shown in Su et al., 2015)

Table 4(on next page)

Ranking of the four tested topological configurations (three rooting scenarios, and scenario 4 constraining the topology of Su et al. 2015)

Ranking is based on marginal likelihood estimates (MLE) and Bayes factors (BF), calculated using two approaches, stepping-stone and path-sampling, implemented in Beast (Baele et al. 2012, 2013)

Table 4. Ranking of the four tested topological configurations (three rooting scenarios, and scenario 4 constraining the topology of Su et al. 2015) based on marginal likelihood estimates (MLE) and Bayes factors (BF), calculated using two approaches, stepping-stone and path-sampling, implemented in BEAST (Baele et al. 2012; Baele et al. 2013)

Rank	Scenario	Stepping-stone		Path-sampling	
		MLE	BF	MLE	BF
1	Rooting sc. 3 *Tupeia* sister to rest	-29457.1		-29456.0	
2	Rooting sc. 1 *Nuytsia* sister to rest	-29461.0	7.87	-29460.0	8.08
3	Scenario 4 (Su et al. 2015)	-29464.3	14.53	-29463.3	14.61
4	Rooting sc. 2 (Lorantheae sister to rest)	-29466.3	18.54	-29465.7	19.43